VOLUME 19, 1957/58, No. 10 pp. 273-300 Published 30th April 1958

Philips Technical Review

DEALING WITH TECHNICAL PROBLEMS
RELATING TO THE PRODUCTS, PROCESSES AND INVESTIGATIONS OF
THE PHILIPS INDUSTRIES

MONITORING, CONTROL AND SAFETY EQUIPMENT FOR A NUCLEAR REACTOR OF THE SWIMMING-POOL TYPE

II. FURTHER DESCRIPTION OF CERTAIN COMPONENT UNITS

by F. E. L. ten HAAF, G. KLEIN and F. J. SCHIJFF.

621.316.7:621.039.4

The design of the auxiliary electronic equipment for a nuclear reactor involves problems which often differ appreciably from those commonly encountered in electronic engineering, and which therefore require a new approach. Some of these problems, which are dealt with below, concern the design of 1) a circuit giving a logarithmic relation between two quantities over a range of many decades, 2) a gamma indicator which gives a direct reading of the dose rate and which can also stop the reactor if necessary, and 3) a safety system which provides complete protection in the event of defects occurring in the reactor.

For the purposes of monitoring, control and safety a nuclear reactor requires elaborate equipment, which is largely electronic. In Part I of this article¹) a general description was given of the equipment provided for the research reactor shown in operation last year at the exhibition "Het Atoom" at Amsterdam, and which is shortly to be installed at the Technische Hogeschool, Delft.

We shall deal here in more detail with three units of this equipment: 1) the logarithmic measuring channel for high neutron flux, 2) the gamma indicator, and 3) the safety amplifiers.

Logarithmic measuring channel for high neutron flux

The logarithmic neutron-flux and period meter, type PW X081 (*fig. 1*), which is connected to an ionization chamber in the reactor, is divided, according to its functions, into

a) a logarithmic amplifier,
b) a period amplifier,
c) a relay stage, and
d) various calibration devices.

The logarithmic amplifier must deliver an output voltage which is proportional to the logarithm of the current in the ionization chamber, and therefore to the logarithm of the neutron flux in the reactor. This output voltage causes the deflection of a meter which is provided with a logarithmic scale (to base 10). The scale, calibrated in percentages of the maximum permissible neutron flux, runs from 10^{-4}% to 300%, thus covering $6\frac{1}{2}$ decades. Provision is made for the connection of a recording instrument.

In the period amplifier the output voltage of the logarithmic amplifier is differentiated and the result amplified. This produces a voltage which is inversely proportional to the "period" (time constant) T of the nuclear reaction.

Since the neutron flux N varies exponentially with the time t, i.e.

$$N = N_0 \, e^{t/T},$$

the logarithmic amplifier delivers a voltage proportional to $\ln N$, and therefore proportional to (const. $+ \, t/T$); thus by differentiation with respect to time t a voltage is obtained which is proportional to $1/T$.

The period T can be read directly from a meter having a reciprocal scale and calibrated in seconds. The scale runs from —30 seconds via infinity to +3

---

¹) M. van Tol, Monitoring, control and safety equipment for a nuclear reactor of the swimming-pool type, I. General description, Philips tech. Rev. **19**, 245-257, 1957/58 (No. 9).

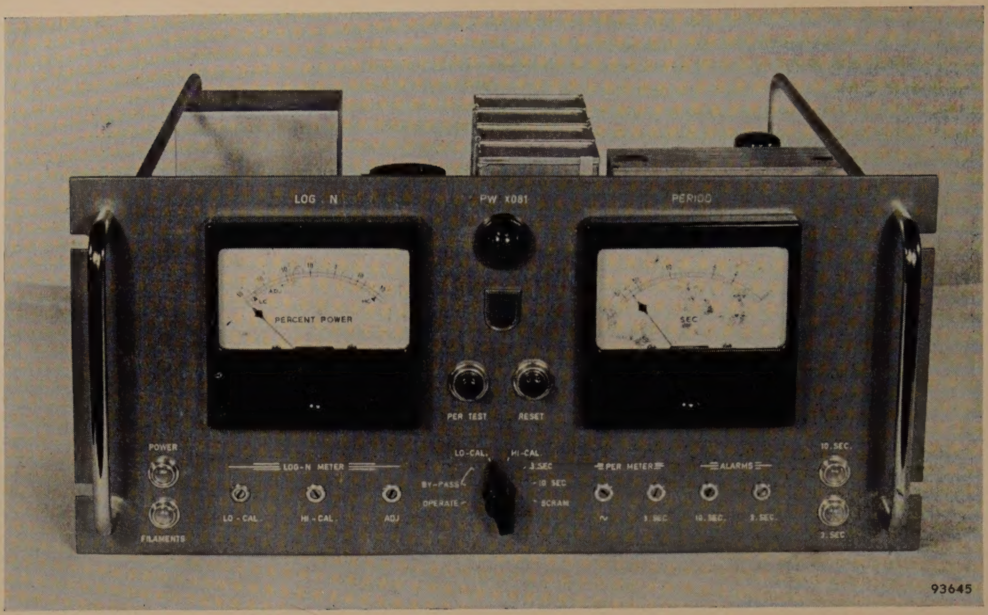

Fig. 1. Unit PW X081 of the logarithmic measuring channel for high neutron flux. Left, the neutron-flux meter with logarithmic scale from $10^{-4}\%$ to 300%; right, the period meter with scale from —30 via ∞ to 3 seconds. Below the meters, the correction resistors, adjustable with a screwdriver; between them a switch with eight positions (one operating position and seven calibration and test positions).

seconds (see fig. 10 in Part I). Here, too, a recording instrument can be connected.

The output voltage is fed to a relay stage as well as to the meters. This stage consists of two relays which come into operation as soon as the reactor period drops below 10 and 3 seconds respectively. The relay contacts ensure that the necessary warning signals are given and the appropriate action taken in the control system: when the period drops to 10 seconds the control rod and the safety rods descend deeper into the reactor core. The effect of this is to reduce the neutron multiplication factor k. If, in spite of this, the period goes on dropping and reaches 3 seconds, the safety rods drop right into the core and thereby stop the chain reaction.

By means of a switch and a push-button, certain standard signals can be supplied to the input to check the reading on both meters. Discrepancies can be corrected by adjusting a number of potentiometers.

The logarithmic amplifier

A familiar circuit element with logarithmic properties is the thermionic diode. Over a certain portion of its characteristic — the retarding-field region — the following relation exists between the current I and the voltage V:

$$I = I_0 \exp \frac{eV}{k\Theta}, \quad \dots\dots \quad (1)$$

where I_0 is a characteristic quantity for the cathode, e the electronic charge, k Boltzmann's constant and Θ the absolute temperature of the cathode. Equation (1) is derived from the fact that the electrons have a Maxwellian velocity distribution. The lower limit of the current range in which (1) is applicable is determined by the quality of the vacuum and of the insulation, and the upper limit is determined by the occurrence of space charge.

If (1) be written

$$V = \frac{k\Theta}{e} \ln I - \frac{k\Theta}{e} \ln I_0, \quad \dots\dots \quad (2)$$

a logarithmic indication of the current I is found by measuring the voltage V over the diode. In practice the change in V amounts to approximately 0.2 V when I changes by a factor of 10.

However, a fixed relation between V and I exists only if the cathode temperature Θ is constant. The second term on the right-hand side of (2) is especially sensitive to changes in Θ, since I_0 also increases with Θ. The filament voltage of the diode must therefore be very well stabilized.

This critical sensitivity to variations in the filament voltage can be circumvented by using a triode instead of the diode. With the triode, in the lower region of its grid voltage/grid current characteristic, an analogous exponential relation exists, as in the retarding-field region of the diode. Further, we may write for a triode, quite generally,

$$\delta I_a = S\,\delta V_g + \frac{S}{\mu}\,\delta V_a, \quad \ldots \quad (3)$$

where I_a is the anode current, V_g the grid voltage, V_a the anode voltage, S the slope (transconductance) and μ the amplification factor. When the anode voltage is constant, (3) reduces to

$$\delta I_a = S\,\delta V_g.$$

A logarithmic relationship also exists, therefore, between I_a and I_g, provided at least that S is constant in the region concerned. In practice this region covers about three decades.

To ascertain the effect of a change in the cathode temperature on the functioning of the circuit, let the filament voltage be raised slightly and consider what happens to the anode current, the grid current being kept constant. Analogous to the case of the diode, both I_g and I_a tend to rise owing to the increase in the cathode temperature. However, since I_g is kept constant, the grid voltage must go more negative, and this in turn causes I_a to decrease. Thus, I_a is subjected to two opposing influences, the one tending to increase it and the other to decrease it. Closer investigation shows that these influences largely compensate each other, so that filament voltage variations cause no appreciable change in the anode current. In this case, then, a rough stabilization of the filament is sufficient.

Another method of obtaining a logarithmic characteristic with a triode is to measure the anode voltage at constant anode current as a function of the grid current. In that case, $\delta I_a = 0$, so that (3) changes to

$$\delta V_a = -\mu\,\delta V_g.$$

Provided μ is constant (this region being larger than that in which S is constant), proportionality thus also exists between δV_a and $\ln(\delta I_g)$. In a manner analogous to that described above, changes in filament voltage are again compensated. A resistance R_a, large with respect to the internal resistance μ/S of the triode, connected to a fixed positive potential (*fig. 2*), as is usual in voltage amplifiers, ensures a practically constant anode current I_a.

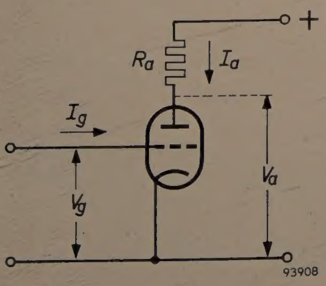

Fig. 2. A logarithmic relation exists between the anode voltage V_a and the grid current I_g of a triode operating in the lower region of its characteristic, at constant anode current I_a. The anode current is here kept approximately constant by the high resistance R_a in the anode circuit.

A tube which is found to be very efficient in the latter circuit is the type E 80 F pentode, operated as a triode. The anode voltage of this tube changes by about 4 V per decade change of grid current. It is not difficult to find a tube of this type whose V_a-I_g characteristic is logarithmic over a grid-current range of $6\frac{1}{2}$ decades.

The period amplifier

As stated, the output voltage of the logarithmic amplifier must be differentiated in order to obtain a voltage which is proportional to $1/T$ and therefore a measure of the period T.

A familiar differentiating network, consisting of a capacitance C and a resistance R, is shown in *fig. 3a*. It is not, however, an ideal differentiator, for a discontinuous change in the derivative of the input voltage V_i (*fig. 4a*) does not cause a jump in the output voltage, as in fig. 4*b*, but a more gradual change moving exponentially to its asymptotic value (fig. 4*c*), the time constant being RC. For our purpose this is undesirable, since the period meter is required to follow, with the least possible delay, every change in the derivative of the output voltage from the logarithmic amplifier. The smaller the time constant RC, the shorter the delay. However, a reduction of RC entails a drop in the output voltage V_o (it is obvious that $V_o = 0$ in the extreme case $R = 0$ or $C = 0$).

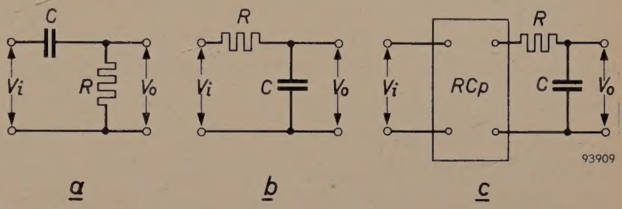

Fig. 3. *a*) Non-ideal differentiator. *b*) Non-ideal integrator. *c*) The non-ideal differentiator (*a*) is equivalent to the ideal differentiator *RC*p and the non-ideal integrator (*b*) in cascade.

The following considerations will help to make this clear. For the differentiating network in fig. 3*a* the differential equation relating the output voltage V_o and the input voltage V_i is

$$V_o + RC\frac{dV_o}{dt} = RC\frac{dV_i}{dt},$$

or, replacing d/d*t* by the Heaviside operator p:

$$V_o = \frac{1}{1+RC\mathrm{p}}\,RC\mathrm{p}V_i, \quad \ldots \ldots \quad (4)$$

whereas for an ideal differentiator

$$V_o \propto \mathrm{p}V_i.$$

For the analogous integrating network (fig. 3*b*):

$$V_o + RC\mathrm{p}V_o = V_i,$$

hence

$$V_o = \frac{1}{1+RC\mathrm{p}}\,V_i. \quad \ldots \ldots \quad (5)$$

Comparing (4) with (5), we see that the only difference consists in the factor RCp, which occurs in (4) but not in (5). This means that (4) corresponds to two networks in cascade, the first being an ideal differentiator RCp and the second the integrator from fig. 3*b*. In other words, fig. 3*c* is equivalent to fig. 3*a*.

It is clear from fig. 3*c* that the smaller R and C become, the closer is the approximation to an ideal differentiator, but it follows from (4) that making RC smaller causes the output voltage V_o to decrease.

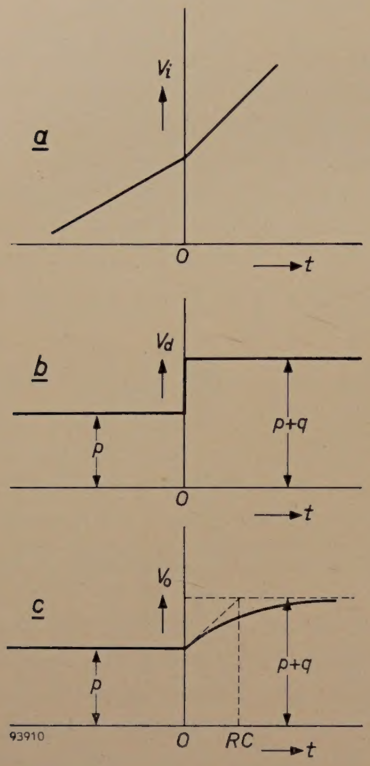

Fig. 4. *a*) Voltage V_i linear with time t, but with a discontinuity in the derivative at $t = 0$:

$$t < 0 \;.\;.\;.\; V_i = pt,$$
$$t > 0 \;.\;.\;.\; V_i = (p + q)t.$$

b) Output voltage V_d of an ideal differentiator whose input voltage has the form shown in (*a*).
c) Output voltage V_o of a non-ideal differentiator as in fig. 3*a*, with input voltage of the form (*a*). The output voltage for $t > 0$ is given by

$$V_o = RC\left[p + q\left\{1 - \exp(-t/RC)\right\}\right].$$

When the period T is 10 seconds, the logarithmic amplifier delivers a voltage which increases by about 0.2 V per second. If we take for RC a value of, say, 0.1 second (the time constant should certainly not be much larger), then, where $T = 10$ seconds, the output voltage of the differentiator is only 20 mV. This is too low for operating the relay stage, for which reason an amplifier is interposed. This consists of two stages (*fig. 5*), the second being a triode cathode follower.

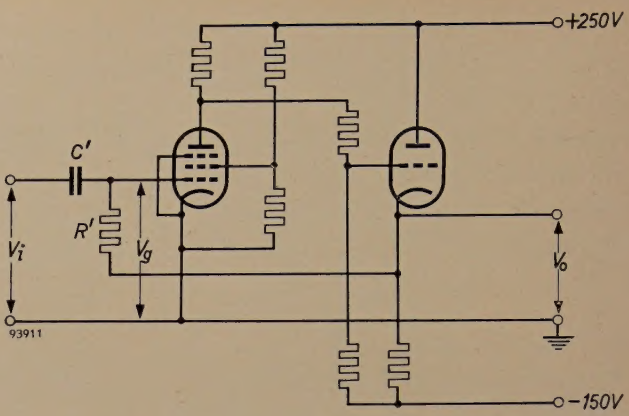

Fig. 5. Differentiator (C' and R') with amplifier. R' is connected to the output (triode cathode follower).

If this amplifier were simply to be placed behind the differentiator (*fig. 6a*), its output voltage — and consequently the reading on the period meter — would be subject to changes in the amplification. There is a simple way, however, of making the output voltage practically independent of the amplification, namely by connecting the resistor in the differentiator to the output of the amplifier instead of to earth (fig. 6*b*, cf. also fig. 5) and by fulfilling the following conditions:

1) the elements R' and C' of the differentiator should be chosen such that $R'C' = A_0RC$, where A_0 is the nominal value of the amplification and RC the original time constant;
2) the amplification A must be much larger than unity.

Fig. 7b shows the step-function response of a circuit which satisfies these conditions. It can be seen that the output voltage, irrespective of A, approaches the same final value (which is not the case with the circuit in fig. 6*a*; see fig. 7*a*). The way in which the final value is approached now depends on A, but this simply means that the period meter

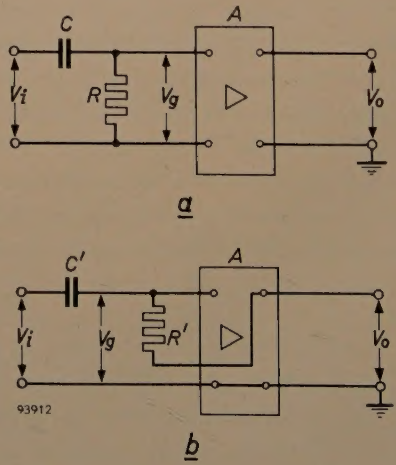

Fig. 6. *a*) Differentiator (C and R) followed by an amplifier with amplification A. The output voltage is proportional to A.
b) Differentiator (C' and R') and amplifier, with R' connected to the amplifier output. Under certain conditions the output voltage is practically independent of A.

reaches its final value rather more quickly or slowly, depending upon A.

The following calculation will serve to explain this. In fig. 6*a* the differentiator has V_i as input voltage and $V_g = -V_o/A$ as output voltage (with this choice of signs, A is a positive number). According to (4),

$$V_o = -A\frac{1}{1+RCp}RCpV_i\,, \quad . \; . \; . \; . \; . \quad (6)$$

which shows the proportional relationship between V_o and A.

In fig. 6*b*, on the other hand, $V_i - V_o$ is the input voltage and $V_g - V_o$ the output voltage of the differentiator, the time constant being $R'C'$. With $V_g = -V_o/A$ and after some manipulation, equation (4) now gives:

$$V_o = -\frac{\dfrac{A}{A+1}}{1+\dfrac{R'C'p}{A+1}}R'C'pV_i\,. \quad . \; . \; . \; . \; . \quad (7)$$

Putting $R'C' = A_0RC$, we may write (7) as

$$V_o = -\frac{A}{A+1}A_0\frac{1}{1+\dfrac{A_0}{A+1}RCp}RCpV_i\,.$$

If, moreover, the amplification is made so large that $A/(A+1) \approx 1$, then

$$V_o \approx -A_0\frac{1}{1+\dfrac{A_0}{A}RCp}RCpV_i\,. \quad . \; . \; . \; . \quad (8)$$

Eq. (8) is of the same form as eq. (6), with the important difference, however, that the constant factor A_0 has taken the place of the fluctuating factor A. Furthermore, RC in the denominator has been replaced by the time constant A_0RC/A, which is not independent of A. As remarked above, however, this is of no practical importance.

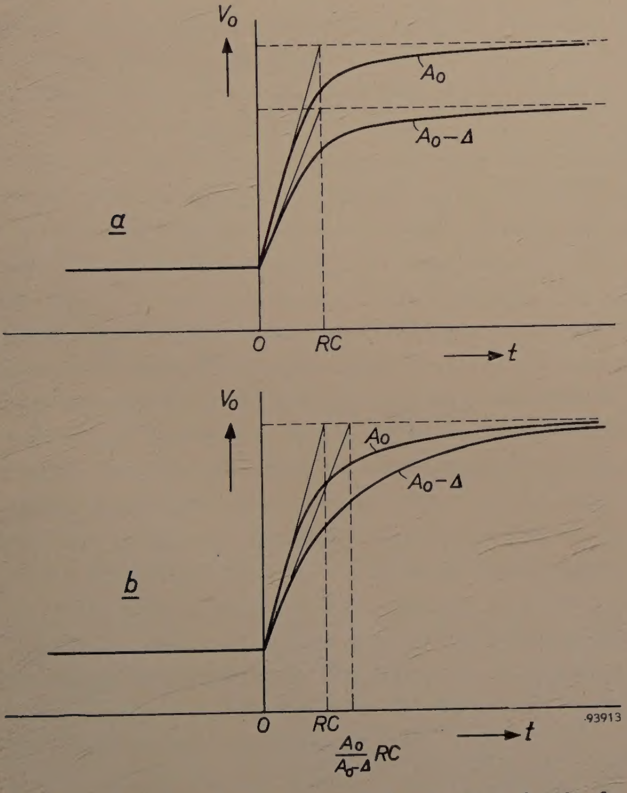

Fig. 7. *a*) Step-function response of the circuit in fig. 6*a*, for two values of the amplification, A_0 and $A_0 - \Delta$. The end values differ, the time constant in both cases is RC.
b) The same for the circuit in fig. 6*b*, with $R'C' = A_0RC$ and $A \gg 1$. Now the time constants differ, but the end values are equal.

The relay stage

The relay stage (*fig. 8*) contains two double triodes operating as so-called Schmitt triggers, *I-II* and *III-IV*. These are so biased that in the absence of a signal from the period amplifier (i.e. with the reactor in the stationary or shut-down state, period $T = \infty$) only *II* and *IV* pass current. In this state the relays A_1 and A_2 are energized; the positions of contacts a_{11}, a_{12}, a_{21}, a_{22} and a_{23} are then the reverse of those drawn in fig. 8.

When the neutron flux increases, T has a finite positive value and the period amplifier delivers a positive output voltage, which is higher the shorter the period. By means of potentiometers P_1 and P_2 respectively, each of the circuits can be so adjusted as to make the loop gain greater than 1 at a given value of T. For the pair *I-II* this point is fixed at $T = 10$ seconds. When this is reached the circuit triggers over into the state in which *I* is conducting and *II* is cut off. The relay A_1 cuts out and contact a_{12} opens. As a result, a warning signal is given on the control desk, and via the intermediary of the servo-mechanism the control rod and the safety rods in the reactor start descending to counteract any further increase in the neutron flux.

If, nevertheless, the period goes on becoming shorter and falls to 3 seconds, *III* becomes conducting and *IV* is cut off. The effect of this is to open contact a_{23}, which interrupts the current to the magnets. As a result, the safety rods drop into the core and the reactor is stopped. At the same time, contact a_{22} opens and a warning signal is given. Moreover, contact a_{21} breaks the anode lead to *IV*, so that relay A_2 can only be actuated again when button *D* is depressed.

The calibration devices

By means of an eight-position switch (fig. 1) certain calibrations and checks can be carried out. As soon as the switch is turned from the measuring (normal) position, a red pilot lamp lights up on the front panel; at the same time a contact is closed which switches on a signal elsewhere, in this case on the control desk. To make calibration possible while the reactor is in operation, in positions 2 to 7 the relay contacts a_{12}, a_{22} and a_{23} are short-circuited (if they were open they would switch on the safety amplifiers and start the servomotors). All calibration adjustments can be made at the front panel with a screwdriver.

The positions of the switch are the following:

1) Normal position (measuring position).
2) In this position everything functions normally, except that the relay contacts mentioned are short-circuited. This is necessary to prevent a false alarm from being sounded when switching back from the calibration positions to the measuring position.
3) As (2), but now the period meter is also short-circuited.
4) Here a known current (10^{-10} A) is fed to the logarithmic amplifier, which should produce a reading on the meter of $2 \times 10^{-4}\,\%$ of full power.

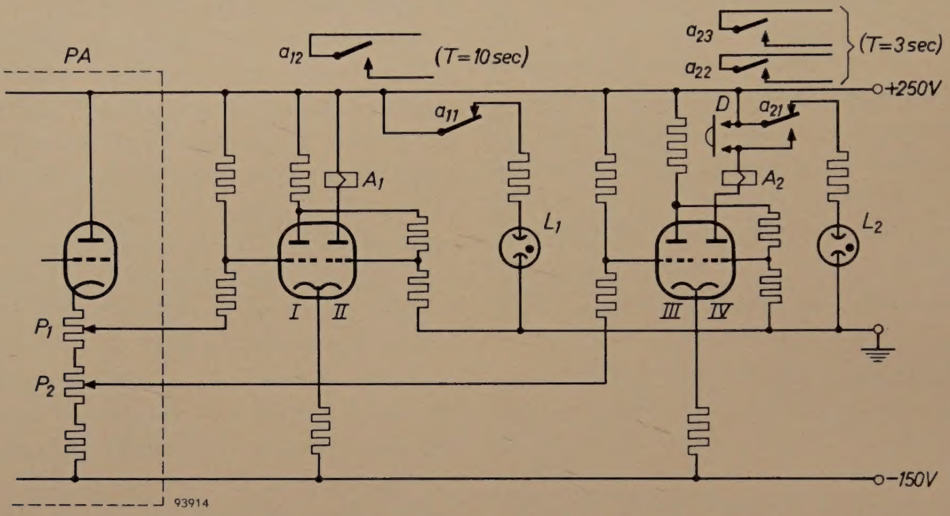

Fig. 8. Relay stage. When the period amplifier *PA* supplies no signal ($T = \infty$), the right halves (*II*, *IV*) of the two double triodes both pass current and the relays A_1 and A_2 are energized; the positions of contacts a_{11}, a_{12}, a_{21}, a_{22} and a_{23} are then the reverse of those shown here. If T drops to 10 seconds, *I* becomes conductive and *II* is cut off; a_{11} closes, a_{12} opens. If T drops to 3 seconds, *III* becomes conductive and *IV* is cut off; a_{21} is switched over, a_{22} and a_{23} are opened. The value of T at which these operations take place can be adjusted with potentiometers P_1 and P_2 in the period amplifier. L_1 and L_2 are neon lamps which indicate the tripping of the relays.

5) As (4), but the current is now 10^{-5} A, and the calibration point lies at 20% of the full power.
6) When the button "Period test" is depressed, a voltage linear with time appears across the input of the period amplifier, the rate of increase corresponding to $T = 3$ seconds. The period meter should now indicate 3 seconds. At the same time the relay circuit *III-IV* triggers; this is indicated by the lighting-up of the neon bulb L_2 (fig. 8).
7) As (6), but now with a voltage increasing at a rate corresponding to $T = 10$ seconds. The neon bulb L_1 (fig. 8) lights up to indicate that the circuit *I-II* has triggered.
8) As (6), but now the relay contacts are no longer short-circuited. This is for checking whether the connections with the safety amplifiers and the servomotors are in order.

The gamma indicator

A nuclear reaction is accompanied by the generation of gamma rays. These rays are a hazard to the health of persons exposed to them. For this reason, and also to indicate the presence of leaks in the fuel elements, a constant check is kept on the intensity of the gamma radiation around the reactor; at the exhibition "Het Atoom" this was done at three positions. If the gamma radiation exceeds a certain intensity, the reactor is automatically shut down ("slow scram") and at the same time a warning signal is given.

Gamma rays, like X-rays, have the property of forming ions in the material through which they pass. The röntgen unit, used to express dosage of X-rays and gamma rays, is defined on the basis of this property. The röntgen is defined as follows (Report International Commission on Radiological Units, 1956): "One röntgen (1 r) is the exposure dose of X- or gamma radiation such that the associated corpuscular emission per 0.001293 gramme of air produces, in air, ions carrying one electrostatic unit of quantity of electricity of either sign". (0.001293 gramme is the mass of 1 cm^3 of dry atmospheric air at 0 °C and 760 mm of mercury pressure.)

The International Commission for Radiological Protection has recommended that the dose rate (dose per unit time) received by persons exposed to radiation in their work should not exceed 0.3 r per week [2]).

---

[2]) See Philips tech. Rev. **16**, 136, 1954/55.

So far as is known, a normal person exposed to such a dose rate will suffer no harmful effect at any time in his life. In the case of the reactor at the Amsterdam exhibition it was assumed that the operating personnel could be exposed to the radiation for 30 hours a week maximum. It was therefore stipulated that at no accessible place should the dose rate exceed 10 milliröntgens per hour (10 mr/h). For comparison it may be noted that the dose rate of cosmic radiation at sea level is approximately 0.01 mr/h, i.e. about 1/1000 of the above stipulated limit.

The gamma detector

For detecting the gamma rays an ionization chamber is used, consisting of a thin-walled steel cylinder of 800 cm^3 volume, filled with argon under 15 atm pressure [3]). The ions released by the gamma rays in the gas are removed by an electric field applied between a central electrode and the wall. The strength of the field ensures that almost no ions are lost by recombination (argon as a filler gas has the advantage over air of allowing the necessary field strength to be reached at a low voltage). The field strength is not so high, however, as to enable new ions to be formed by collisions with the gas atoms. The current obtained is thus dependent solely on the dose rate.

If the ionization chamber were filled with air at 1 atm and 0 °C, and if the volume were 1 cm^3, the gamma rays at the maximum permissible dose rate of 10 mr/h would liberate per hour a charge of 0.01 e.s.u. $= 3.33\times10^{-12}$ coulomb. The maximum detector current would then be $3.33\times10^{-12}/60^2 \approx 10^{-15}$ A. In the actual detector this current is a great deal higher, namely (ignoring, among other things, the wall effect) by a factor of 800 due to the larger volume, a factor of 15 due to the higher pressure, and a factor of about 1.25 due to the use of argon instead of air (which is thus an incidental advantage of argon over air). The detector current at the maximum permissible dose rate is therefore approximately:

$$800\times15\times1.25\times10^{-15} \approx 1.5\times10^{-11} \text{ A}.$$

At the position of the ionization chamber the radiation has already covered an appreciable distance through water and possibly through concrete, so that what is left is practically only hard radiation. The power of hard-radiation quanta to dislodge electrons from the gas atoms is proportional to the number of electrons per cm^3, and therefore to the number of gas atoms per cm^3 and to the atomic number of the gas. The atomic number of nitrogen is 7, that of oxygen 8 (average for air: 7.2), and that of argon 18. Since 1 cm^3 argon at 15 atm contains just as many atoms as there are molecules in 1 cm^3 air at 15 atm, and since this number of molecules is half as large as the number of N and O atoms, the gain by using argon instead of air is $18/(2\times7.2) = 1.25$. (This simplified calculation does not include all the factors of influence.)

The minimum detector current required to be measured corresponds to the dose rate of cosmic radiation (approx. 0.01 mr/h), viz. a current of the order of 10^{-14} A.

Measurement of the detector current

For measuring the gamma-detector current the tetrode electrometer tube 4066 is used. The control grid is connected only to the central electrode of the gamma detector. The tube thus operates with a grid current which is equal and opposed to the detector current (the insulation is so efficient that the maximum leak current is of the order of 10^{-15} A and may therefore be neglected).

At this very weak grid current (10^{-14}-10^{-11} A, entirely in the exponential region), we again find that a change in the grid voltage δV_g is proportional to the logarithm of the associated change in the grid current, δI_g. Since δV_g results in a proportional change, δI_a, in the anode current, δI_a is proportional to log (δI_g). The grid-current changes, which are equal to the detector-current changes and thus proportional to the dose rate, can be read on a logarithmic scale on a moving-coil meter in the anode circuit (the relatively high quiescent anode current is compensated in the meter by a simple circuit arrangement). A logarithmic scale has the advantages, mentioned earlier in this article, that it covers many decades (so that one measuring range suffices, reducing the risk of mistakes in reading) and that the relative sensitivity is equal over the whole scale.

The electrometer tetrode type 4066 is a subminiature tube whose second grid acts as control grid. The first grid serves as space-charge grid, for which purpose it receives a constant positive voltage of a few volts.

The tube is mounted inside the gamma detector. The great advantage of this is that the connection of the central electrode to the control grid does not have to be led through the steel wall of the detector, which means that the part of the circuit which must be highly insulated is situated in a dry and unchanging environment. Lead-ins are now necessary, of course, for the supply to the other electrodes, but no particularly high insulation resistance is needed for these.

---

[3]) This gamma detector was designed and built by K. van Duuren and co-workers, for the Philips Research Laboratories, working at the synchrocyclotron at Amsterdam.

Transistorized light-relay

Since the anode current of the electrometer tube is too weak to energize a relay directly, a light-relay device is used.

At the end of the scale of the anode-current meter, at 10 mr/h, an opening is made in the dial. Through this opening, light from an electric bulb falls on to a transistor, which then passes a current between emitter and collector powerful enough to actuate a relay. As soon as the light is intercepted by the needle, however, the transistor current drops practically to zero; the relay then cuts out, and as a result the reactor is stopped and an alarm device set in operation. (In this arrangement, then, an amplifier, as would be needed with a normal photocell, is unnecessary.) To check whether the system is functioning correctly, a radioactive specimen can be placed near one of the ionization chambers.

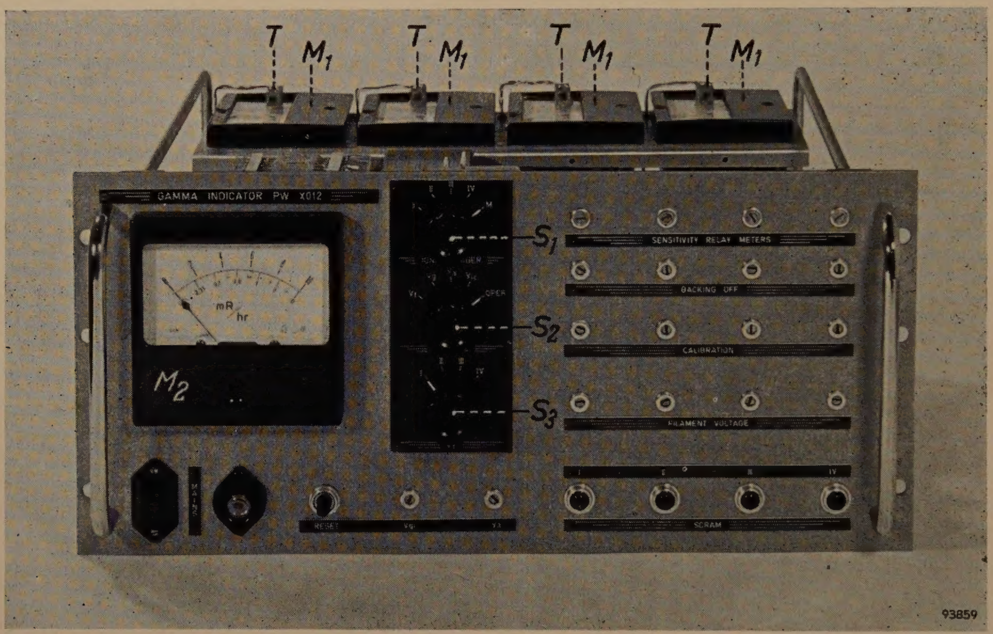

Fig. 9. Gamma-indicator unit PW X012. Above: the four light-relay meters M_1 on which are mounted transistors T. On the front panel: meter M_2 indicates the dose rate, or functions as a test voltmeter, depending on the position of switches S_1, S_2 and S_3.

In principle, every transistor is sensitive to light. In ordinary operation this phenomenon would be troublesome, which is why normal transistors are protected against light by a coating of lacquer. The OCP 71 transistors used here have no such coating, but are otherwise of the normal type.

Circuit of the gamma indicator

The panel of the gamma-indicator unit is shown in *fig. 9*. The circuit is equipped for four ionization chambers. The four light-relay meters M_1 can be seen with their transistors T. These meters give full deflection at 10 μA. The meters are horizontal because if such sensitive instruments were to be mounted upright (with the axis of the moving coil horizontal), the needle might easily stick at the beginning or the end of the scale. To facilitate the reading, however, a further meter M_2 is mounted on the front panel, which can be switched to each of the four channels (if this meter should stick, the safety measures are not affected).

The circuit of one channel can be seen in *fig. 10*. The correction resistor R_1 serves for matching the deflection of meter M_1 to that of M_2 from which the reading is made.

The relative sensitivity is 1 μA per factor 2, i.e. the current through M_1 increases by 1 μA when the dose rate is doubled. There should be full deflection (10 μA) at 10 mr/h. The range of the scale is therefore ten factors of 2, i.e. $2^{10} \approx 1000$. The zero point of the meter thus corresponds to 0.01 mr/h (cosmic radiation). The required relative sensitivity of 1 μA per factor 2 can be adjusted by regulating the voltage on the first grid (with series resistor R_3) and if necessary by varying the filament current (with resistor R_4).

After this adjustment, an absolute calibration is necessary, that is to say the anode current must be compensated in such a way that the meter will indicate the actual dose rate at the position of the detector. For this calibration a radioactive source of known intensity is needed (the intensity may be very low, owing to the high sensitivity of the instrument). The compensation current can be varied with potentiometer P (fig. 10). Like the resistors R_1, R_3 and R_4, P can be adjusted with a screwdriver.

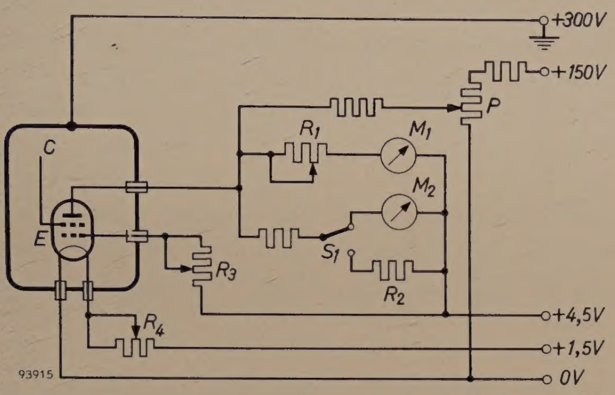

Fig. 10. Diagram of one channel of the gamma indicator. D is the ionization chamber functioning as gamma detector; mounted in it are the electrometer tetrode E (type 4066) and the central electrode C. M_1 light-relay meter. R_1 correction resistor. M_2 meter for reading the dose rate. S_1 switch used either for switching M_2 successively into the four channels or for measuring the supply voltages. R_2 equivalent resistor for M_2. P potentiometer for adjusting the compensation current. R_3 resistor for varying the voltage on the space-charge grid of the electrometer tube. R_4 filament resistor.

The meter M_2 can be switched into each of the four measuring channels by means of a five-position switch. An equivalent resistance R_2 takes the place of the meter in the channels in which the meter is not being used. The fifth position serves for checking the supply voltages on the same meter. These are stabilized such that mains voltage fluctuations up to 10% have no significant effect on the reading.

The steel detector cylinders are earthed for safety reasons. The other parts of the apparatus are thus at a potential of about —300 V with respect to earth.

Measurement with different radiation sources

Because of the use of argon instead of air in the ionization chambers, it might be feared that the ion yield would depend in a different way on the hardness of the radiation. Since, in our case, only hard radiation is present near the ionization chambers (the softer rays are mostly absorbed in the water and in the concrete), any such effect may be expected to be very small. To verify this, we carried out an experiment with two different radiation sources: cobalt (radiations of 1.1 and 1.3 MeV) and caesium (radiation of 0.66 MeV). At these energies argon was found to be practically equivalent to air.

After all specimens had been removed — leaving only the cosmic radiation — the meter reading was 0.01 mr/h. This demonstrates the highly effective insulation of the central electrode and the control grid.

The safety amplifiers

The safety system has two ionization chambers of its own. The current from each is fed to two "safety amplifiers", which function as relays. The system also comprises a square-wave generator (2000 c/s) and two rectifiers, one of which supplies the direct voltage (300 V) for the square-wave generator and for the ionization chambers, and the other the energizing current for the electromagnets from which the safety rods are suspended. All these parts are mounted in the safety unit type PW X086 [4]). If the current from one of the ionization chambers is too high — owing to the neutron flux being too high — one of the safety amplifiers interrupts the magnet currents, causing the safety rods to fall and thereby stopping the reactor.

The ionization chambers (of American manufacture) employed in the safety channels are of the parallel circular plate type ("PCP"). The electrodes consist of a number of circular plates stacked parallel to each other so as to give a large effective surface. The plates are of graphite (a material which does not become highly radioactive under neutron bombardment) covered with a layer of boron enriched with isotope B^{10}. The latter has a large effective cross-section for thermal neutrons. When a B^{10} nucleus absorbs a neutron, an alpha particle (${}_2He^4$) is liberated:

$$ {}_5B^{10} + {}_0n^1 \longrightarrow {}_2He^4 + {}_3Li^7, $$

and these alpha particles as well as the lithium nuclei cause ionization in the nitrogen with which the chamber is filled. In this way an ionization current is produced which is proportional to the thermal neutron flux.

A simplified circuit diagram of the safety amplifiers is reproduced in *fig. 11*. The anode circuit of a thyratron Th contains a relay coil A and is supplied with a square-wave voltage of frequency 2000 c/s. Through resistor R_1, which connects the grid with the cathode, a current I flows from the ionization

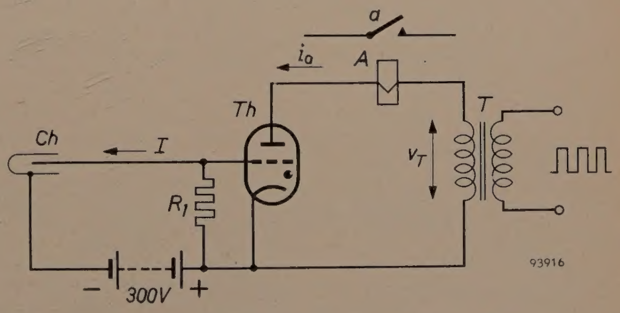

Fig. 11. Simplified circuit of safety amplifier. The current I from the ionization chamber Ch produces across resistor R_1 a voltage which, when greater than a critical value, prevents the thyratron Th from igniting. The relay A is then de-energized and contact a opens, the result of which is to stop the reactor. The anode circuit is supplied with a square-wave voltage via transformer T.

---

[4]) At the exhibition "Het Atoom" a safety unit of American manufacture was used. In Delft this will be replaced by a PW X086 unit.

chamber *Ch*. The grid voltage is thus a direct voltage proportional to *I*, hence proportional to the neutron flux at the position of the ionization chamber. As long as *I* is smaller than a critical value, the thyratron passes a constant current during half of each cycle — owing to the square-wave form of the supply voltage (*fig. 12*) — and this current actuates the relay. If *I* exceeds the critical value, the grid voltage goes so negative that the thyratron can no longer ignite, and consequently the relay cuts out; the contact *a* (fig. 11), through which the current for the electromagnets passes, then opens and the safety rods fall into the reactor.

In all there are four identical safety amplifiers, two of which are connected to one ionization chamber and two to the other, as indicated in *fig. 13*. In this figure one of the amplifiers is shown in more detail. The thyratron, type PL 2D21, has a screen grid, which is connected to the cathode. The relay coil is shunted with a capacitor *C* for by-passing the alternating-current component of the anode current. *G* is the rectifier which supplies the electromagnets *M*. The relays *A'*, *A''*, ... have two sets of contacts, viz. a_2', a_2'', ..., which interrupt the direct current, and a_1', a_1'', ... which, as an extra precaution, cut out the rectifier at the alternating-current side. Each relay also has a contact (not shown) which causes a red lamp to light up on the control desk for as long as the relay is not energized.

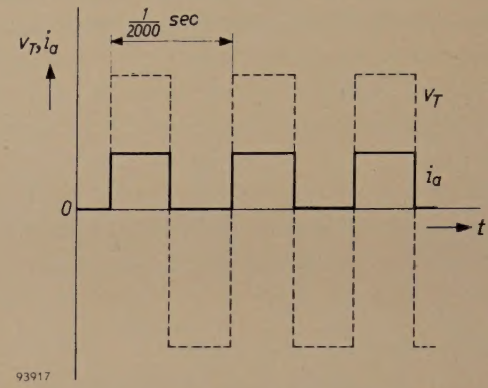

Fig. 12. Supply voltage v_T and anode current i_a of the thyratron in fig. 11, as a function of time *t*.

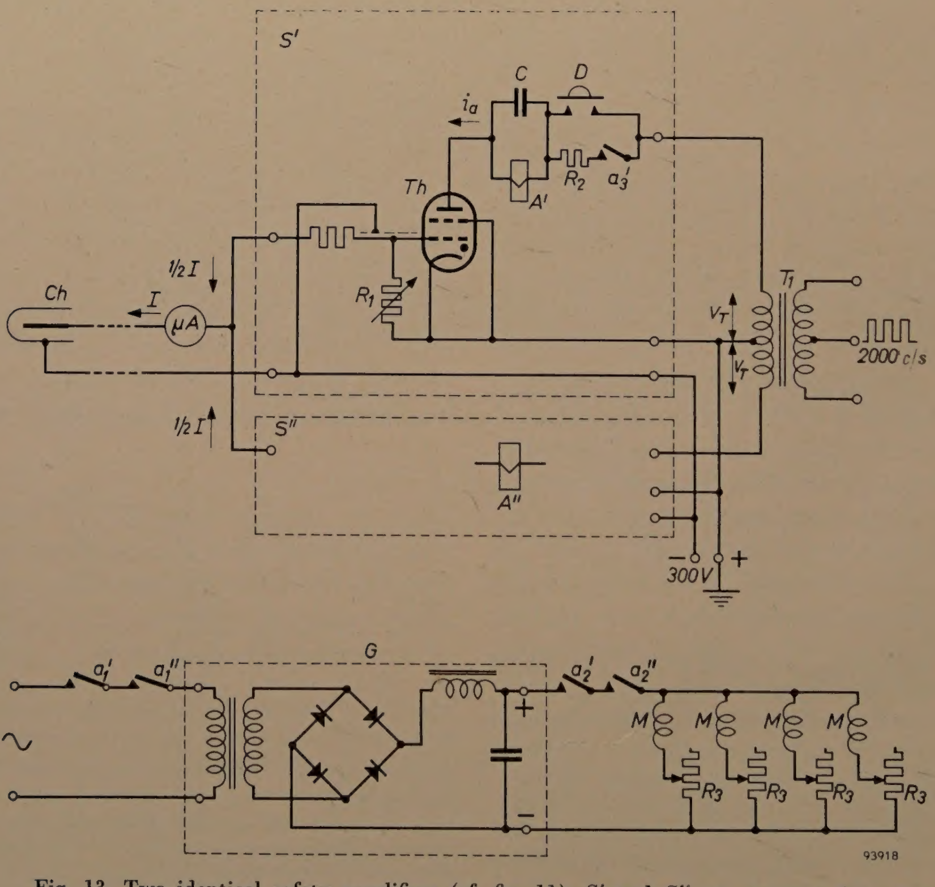

Fig. 13. Two identical safety amplifiers (cf. fig. 11), *S'* and *S''*, are connected to one ionization chamber *Ch*. R_1 is a variable resistor for adjusting the current *I* at which the safety system operates. *Th* thyratron PL 2D21. *A'* relay type T 51 C, with contacts a_1', a_2' and a_3'; the contacts a_1'' and a_2'' belong to the corresponding relay *A''* in *S''*. *C* capacitor (A.C. shunt). R_2 series resistor, short-circuited by push-button *D*. T_1 power transformer which supplies a square-wave voltage of 2000 c/s to both amplifiers. The rectifier *G* supplies the four electromagnets *M* via variable resistors R_3.

The current I at which the amplifiers enter into operation (the "scram point") can be adjusted by variable resistors R_1. These resistors also serve to correct for the spread in the characteristics of tube PL 2D21.

After the reactor is stopped, the current I becomes zero. The thyratrons would now be able to ignite again if their anode circuits were not interrupted by the contacts a_3', ..., which are also opened when the relays cut out. In order to actuate the relays again, push-button D is pressed for a moment, so that contacts a_3', ... are shunted. Since this also short-circuits the resistors R_2, anode currents flow which are somewhat higher than normal, so that the relays cannot fail to be actuated. When D is released, the resistors R_2 are switched in again and the circuit returns to normal.

A photograph of the safety unit is given in *fig. 14*.

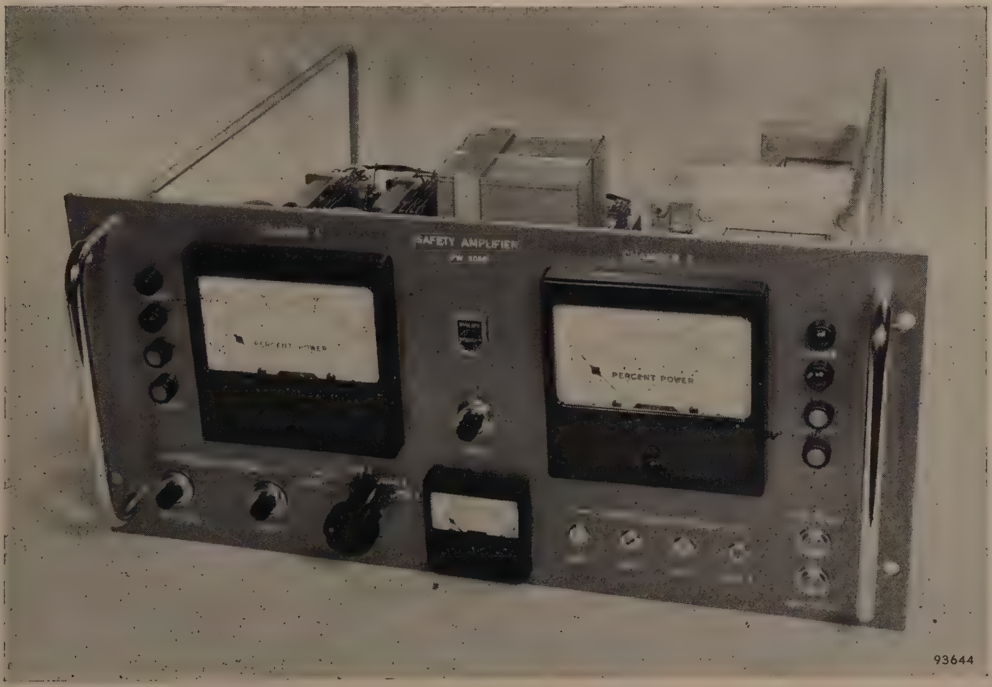

Fig. 14. Unit PW X086 with four safety amplifiers as in fig. 13. The two large meters indicate the current through the ionization chambers and have a relative scale for reading off the percentage power. Between them is a push-button (D in fig. 13) for resetting the amplifier after stoppage. Below: meter for testing the supply voltage and magnet currents, with five-position switch. Further to the left are the test push-buttons for feeding different calibrating currents to the input. Right, screws for adjusting the four resistors to regulate the magnet currents (R_3 in fig. 13).

"*Fail-safe*" *measures and reliability*

An important requirement imposed on a safety amplifier is that, no matter what internal defect arises, safety should not be jeopardized, i.e. any fault in the safety equipment itself must result in the reactor being shut down. In reality this "fail-safe" requirement can never be entirely fulfilled; there is always a chance of faults occurring which do not result in complete shut-down. Safety amplifiers should be so designed as to reduce the risk of such faults to a minimum. On the other hand it is of the utmost importance to avoid *unnecessary* stopping of the reactor: it is a nuisance and time-consuming in the case of a research reactor but can have serious economic consequences in the case of a power reactor. The safety system must therefore reach a very high standard of *reliability*. This means that only components of the highest quality should be used, and that the apparatus should be as simple as possible.

Safety can also be improved by duplicating the installation; in our case two ionization chambers are employed and four safety amplifiers. Naturally, this slightly increases the chance of unnecessary stoppage.

Closer examination [5]) shows that the chances of failure are multiplicative and the chances of unnecessary stoppage additive. Thus, the situation is always relatively improved by duplication.

In the U.K., for example, a system has been adopted with three safety systems, on the recommendation of the Atomic

---

[5]) E. Siddall, Reliable reactor protection, Nucleonics **15**, No. 6, 124-129, 1957.

Energy Research Establishment at Harwell; these are so arranged that when only one of them comes into operation, merely an alarm is sounded, and the reactor is stopped only when two (or all three) operate. With this system the chance of unnecessary stoppage is much smaller than with a duplicated installation, while in both cases the chance of failure is of the same order.

In *Table I* a summary is given of defects that may occur in the safety amplifiers in unit PW X086 and of their consequences. From the notes appended to this table, it can be seen that the amplifiers are to a high degree "fail-safe". The fact that this result is achieved with relatively few components adds substantially to the reliability of the system.

A further measure adopted to prevent failure of the amplifier is that the screening of the control-grid leads is not connected to earth but to a point of —300 V potential (fig. 13); this does not detract from the screening, since the source of 300 V has a low impedance, and it has the advantage that the relay is de-energized in the event of a short-circuit between a point of the circuit and the screening.

The advantage of using a common direct-voltage source for the ionization chambers and the square-wave generator is that failure of this source also de-energizes the (relay the square-wave voltage having disappeared). As can be seen from fig. 13, no point in the circuit has a positive potential with respect to the cathode; there is therefore no possibility of a positive direct voltage appearing on the anode as a result of a short-circuit — which would keep the thyratron ignited and the relay energized.

Table I. Possible defects in the safety amplifiers, and their consequences.

Resistor R_1 interrupted	relay de-energized
,, ,, short-circuited	relay stays energized
μAmmeter interrupted *)	,, ,, ,,
,, ,, short-circuited	no effect
Relay coil open-circuit	relay de-energized
,, ,, short-circuited	,, ,,
Capacitor C interrupted	,, ,,
,, ,, short-circuited	,, ,,
Resistor R_2 interrupted	,, ,,
,, ,, short-circuited	,, ,, **)
Thyratron: leak	,, ,,
,, : interruption filament current	,, ,,
,, : ,, control grid (g_1)	,, stays energized
,, : ,, screen grid (g_2)	,, de-energized
,, : ,, anode (a) . . .	,, ,,
,, : short-circuit cathode (k)-g_1 ***)	,, stays energized
,, : ,, ,, k-g_2	no effect
,, : ,, ,, k-a ***) . . .	relay de-energized
,, : ,, ,, g_1-g_2	,, stays energized
,, : ,, ,, g_1-a ***) . . .	,, ,,
,, : ,, ,, g_2-a	,, de-energized
Failure of 2000 c/s generator	,, ,,
,, ,, 300 V supply	,, ,,

*) The chance of interruption is very slight, since the meter is fitted with a shunt.

**) Since, with short-circuited R_2, the anode current is higher than usual, the relay opens more slowly and only at a higher ionization current I.

***) The construction of tube PL 2D21, and the wiring are such that short-circuiting of k-g_1, k-a and g_1-a is practically impossible.

Another important point worth mentioning is the deliberate use in the circuit of a rectifying element (the thyratron) enabling the D.C. relay to be energized from a source of alternating voltage. In the event of a short-circuit between anode and cathode, or between anode and screen grid, the relay will therefore be de-energized.

As stated, the safety amplifiers are fed by a square-wave voltage, the reason being that the anode current pulses then always last for half a cycle and thus the average anode current is independent

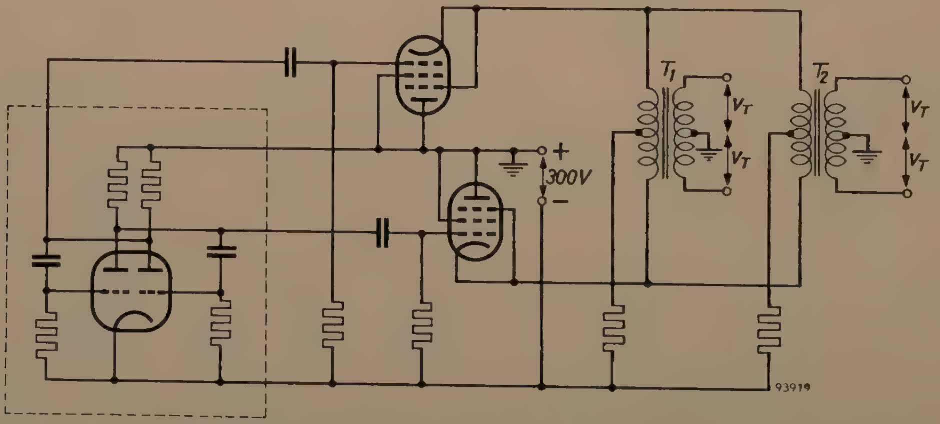

Fig. 15. Circuit diagram of 2000 c/s square-wave generator. Inside the broken lines is the multivibrator with double triode E 90 CC. Right, balanced push-pull output stage with two pentodes EL 34 giving cathode-follower output. T_1 and T_2 are the output transformers, each of which supplies two safety amplifiers.

of the grid voltage. The frequency is chosen as 2000 c/s because one complete cycle can elapse before the relay current is interrupted, 2000 c/s being equivalent to 0.5 millisecond. Added to the 4 milliseconds opening time of the relay (type T 51C), this gives a total time of 4.5 milliseconds. "Less than 5 milliseconds" is the requirement; this time is so short that the falling rods, even in the most unfavourable case, adequately slow down the reaction.

Finally, some words on the test device and on the square-wave voltage generator.

Test device

The operation of the safety system can be tested as follows. Pressing a button causes a specific direct current to be fed to the input of the safety amplifier; when this is done the relay should become de-energized. By pressing another button a current about 10% lower is fed to the input; the relay should then stay energized.

Both currents are taken from the direct-voltage source of 300 V and can be adjusted with a variable resistor inside the unit.

The square-wave voltage generator

The square-wave voltage of 2000 c/s is supplied by a generator (*fig. 15*) consisting of a multivibrator and a power amplifier, both fed by a direct voltage of 300 V. The multivibrator (with a double triode E 90 CC) delivers a square-wave voltage (substantially independent of the valve characteristics) of 140 V (280 V peak-to-peak, hence almost the maximum obtainable with 300 V supply voltage). The latter voltage drives a balanced push-pull output stage containing two EL 34 pentodes with cathode follower output. The efficiency of this stage is low, but it has the advantage that variations in tube characteristics have hardly any effect on the voltage gain (which is approximately 1).

There are two output transformers (T_1, T_2), whose primaries are connected in parallel. Each has two secondary windings and supplies two safety amplifiers (see fig. 13). A tight coupling between primary and secondary coils precludes overshoot transients.

Summary. The article describes three component units of the monitoring equipment for the nuclear reactor displayed at the exhibition "Het Atoom" and shortly to be installed at the Technische Hogeschool, Delft. These units are:

1) The logarithmic measuring channel for high neutron flux. Besides an ionization chamber this comprises: a logarithmic amplifier, in which the logarithmic element is a triode operating in the exponential region; a "period amplifier", which supplies a voltage inversely proportional to the period of the reactor; a relay stage, with two relays which open safety contacts when the period drops to 10 and 3 seconds respectively; and various calibrating devices.
2) The gamma indicator, with four ionization chambers of 800 cm^3 volume, filled with argon at 15 atm. The ionization current is measured with an electrometer tetrode 4066, which is mounted inside the ionization chamber to avoid leakage currents. A light-relay utilizing a transistor is actuated by this tube and so trips an ordinary relay.
3) The safety amplifiers, which are designed with "fail-safe" features, i.e. to ensure that the reactor is stopped in the event of any defects in the safety equipment itself; in this way defects in the safety equipment have practically no effect on the safety of the whole, while unnecessary stoppages are avoided as far as possible.

DIRECT OBSERVATION OF WEISS DOMAINS BY MEANS OF THE FARADAY EFFECT

538.614

By cooling a nearly eutectic melt, large plate-like single crystals of the hexagonal compound $BaFe_{12}O_{19}$, the main constituent of ferroxdure, can be obtained. In this process, now in use for some years in the Philips Research Laboratories [1]), extremely thin crystal plates may be obtained under certain conditions. Their thickness is less then a micron and their surface area of the order of one square millimetre. X-ray diffraction photographs of these tiny platelets have shown that they too are single crystals of $BaFe_{12}O_{19}$, with the hexagonal axis perpendicular to the flat surface.

The special interest of these platelets is that they are reasonably transparent to red light. (This is related to the high resistivity of $BaFe_{12}O_{19}$, a characteristic which is due to the fact that all iron ions present in this compound have valency 3. The presence of even small quantities of iron ions of valency 2 besides those of valency 3 will in general cause a much lower resistivity and a strong absorption of light.) The transparency of the platelets opens up an elegant method for the direct observation of the Weiss domains in $BaFe_{12}O_{19}$. The platelet is observed in a polarizing microscope with nearly-crossed nicols. One then sees an image such as those depicted here in *figs. 1-3*.

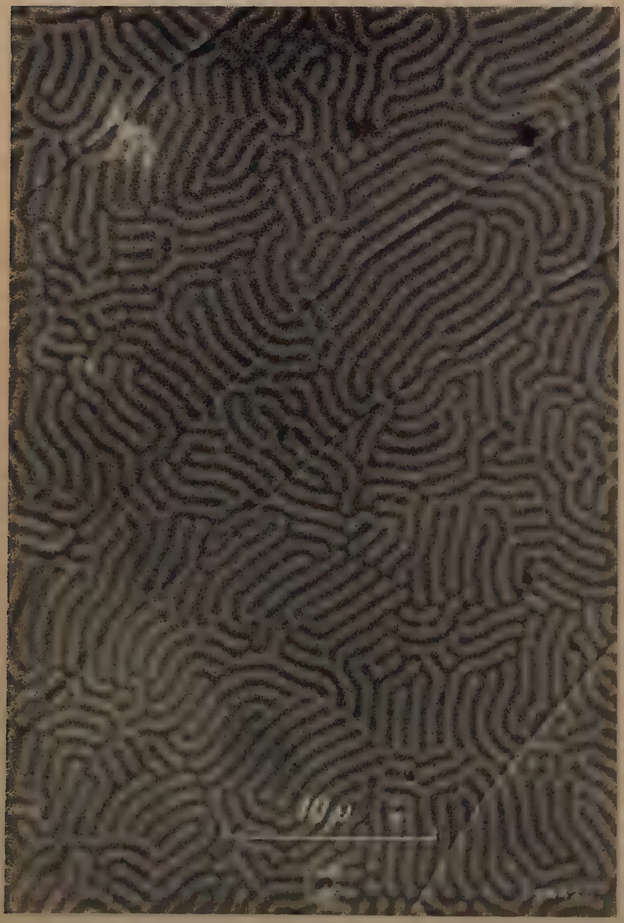

Fig. 1.

Fig. 2.

Fig. 1. Single-crystal platelet (< 1 μ thick) of $BaFe_{12}O_{19}$ in the virgin state, as seen under a polarizing microscope with the nicols not quite exactly crossed. The light and dark bands are elongated Weiss domains.

Fig. 2. The same platelet as in fig. 1, after magnetizing. The domain pattern has assumed a much simpler form. (From scratches and spotty surface faults one can see that this photo represents almost the same region as that in fig. 1.)

---

[1]) A. L. Stuijts, to be published elsewhere.

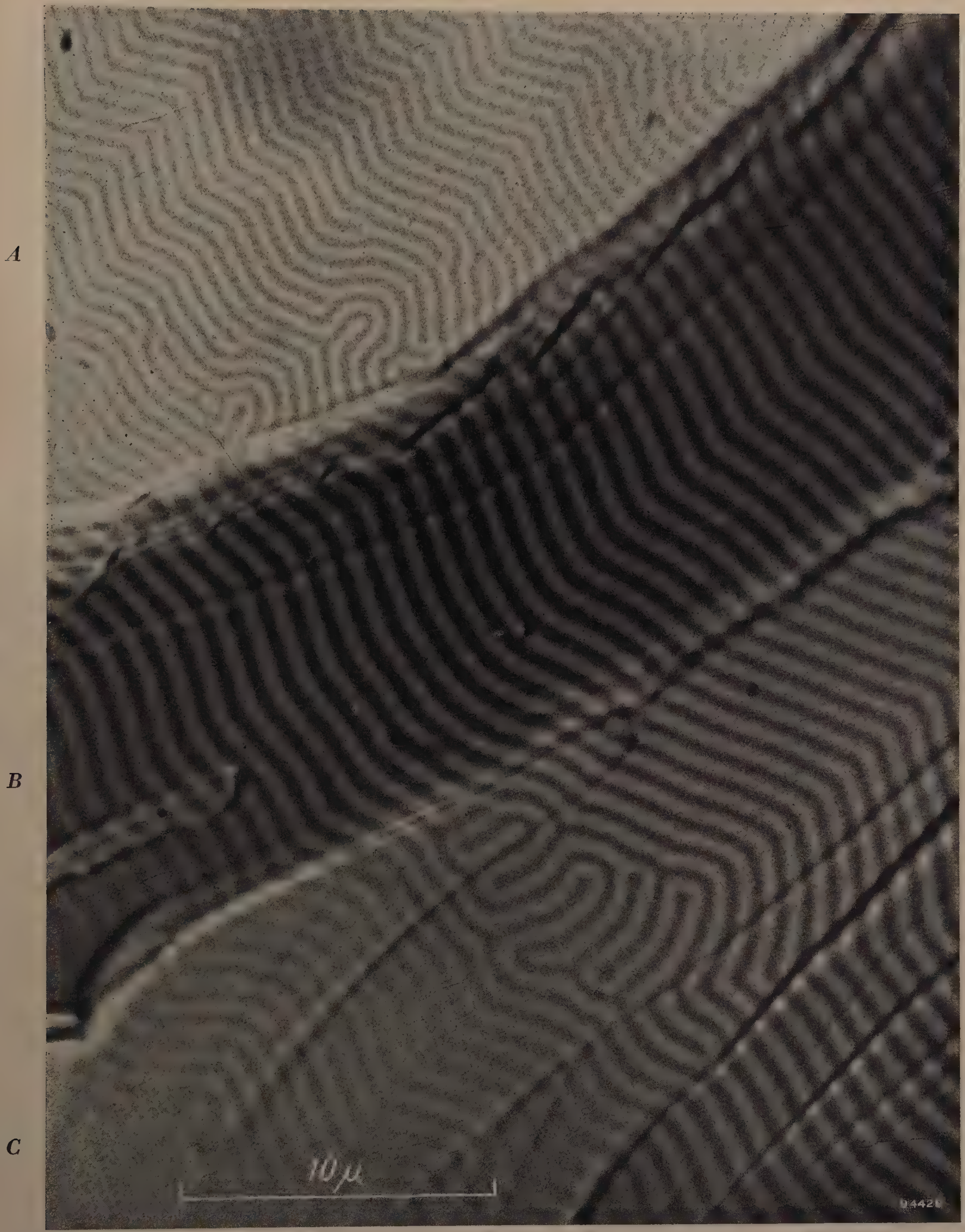

Fig. 3. Similar photo to that of fig. 2, showing another region of the same platelet. Terraced thickening of the specimen can be seen in this region by the dark broad bands across the pattern. The Weiss domains are seen to be wider within these dark bands. The "contraction" of the pattern on passing the boundary from a thick to a thinner place is at some points taken up by dislocation-like imperfections in the pattern.

A brief explanation of the occurrence of these patterns and an indication of some of the details to be seen may be appropriate here.

In each Weiss domain in a ferromagnetic material the magnetic moments of the atoms or ions are parallel aligned, so that in each domain the saturation magnetization exists. The direction of magnetization, which depends on the crystal-shape- or stress-anisotropy, differs from one Weiss domain to another. In $BaFe_{12}O_{19}$ the direction of the magnetization is entirely determined by the very large crystal anisotropy; the preferred direction of magnetization is here the hexagonal axis (c-axis). In the crystal platelets therefore, the magnetization of all Weiss domains is perpendicular to the flat surface, in spite of the high demagnetization factor of the plate form. The Weiss domains are thus magnetized as sketched in *fig. 4*, with the domain walls all perpendicular to the flat surface. Because the magnetization is so strongly bound to the hexagonal axis in $BaFe_{12}O_{19}$, no "closing" domains occur at the surface (i.e. Weiss domains with magnetization parellel to the surface), in contrast with the usual situation in other materials.

If a beam of plane-polarized light is now projected parallel to the hexagonal axis on to such a platelet, a Faraday rotation occurs, of magnitude and sign dependent on the magnetization. Suppose that for one domain the plane of polarization undergoes a rotation described by a right-handed screw; the light passing through an adjacent domain, owing to the oppositely-directed magnetization, will then undergo an equal rotation of its plane of polarization in the opposite direction, i.e. corresponding to a left-handed screw. An analysing nicol is placed in the emerging beam. By placing this not exactly perpendicular to the plane of polarization of the incident beam, the intensity of the rays passing through adjacent, oppositely-magnetized domains will differ slightly; see *fig. 5*. In this way the whole domain pattern becomes visible [2].

The pictures shown in figs. 1-3 were made in this manner. The hexagonal axis of the crystal lies perpendicular to the plane of the photographs. The Weiss domains, with their magnetizations directed alternately upwards and downwards out of the plane of the picture, are seen as light and dark bands. The remarkable labyrinth structure of fig. 1 is the domain pattern in the *virgin state*, as occurs after cooling the material from a temperature above the Curie point. Fig. 2 is a photo of practically the same region as that in fig. 1, taken after magnetizing the specimen in a field of 48 × 10⁴ A/m [6000 oersteds] parallel to the hexagonal axis. The domain pattern has here assumed a much simpler form; the ribbon-like domains are seen as wavy lines. The remanent magnetization of the platelet is practically zero as a result of the very large demagnetization factor with such a thin specimen. This can be seen in the photo since the light and dark bands are equally wide; in the total volume, therefore, their is no surplus of one direction of magnetization over the other.

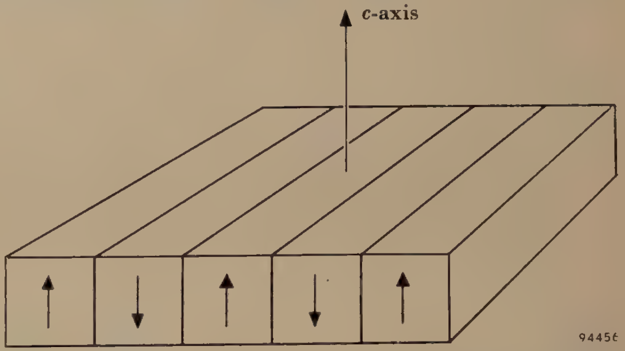

Fig. 4. Schematic diagram showing the configuration of Weiss domains in the single-crystal platelets of $BaFe_{12}O_{19}$. The domain walls are perpendicular to the flat surface of the platelets, parallel to the hexagonal c-axis. The arrows show the directions of the magnetization.

The *width* of the Weiss domains depends on the thickness of the crystal plate. The formation of the domain walls requires a certain energy, proportional to the wall area; on the other hand the magnetostatic energy of the whole body is reduced by the formation of the domain walls. With increasing thickness of the plate the magnetostatic energy becomes smaller, whereas the domain walls would take up more energy owing to their greater area (greater height) if their spacing remained the same. The total energy

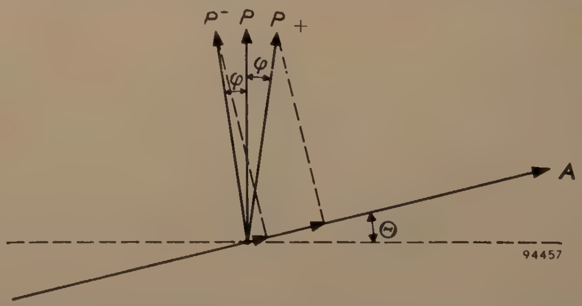

Fig. 5. If P is the direction of polarization of a light beam (here considered incident perpendicularly to the paper), the Faraday effect in one Weiss domain gives rise to a rotation φ to $P+$, while in adjacent oppositely-magnetized domains the same rotation occurs in the opposite sense, to P^-. An analyser set with its transmission direction at A, 90° — Θ from P, attenuates the light with the polarization P^- more than that with the polarization $P+$.

The transmitted intensities are related to each other as $\sin^2(\Theta - \varphi) : \sin^2(\Theta + \varphi)$. Maximum contrast is obtained at $\Theta = \varphi$, but for a small value of φ the transmitted intensity is too small when $\Theta = \varphi$. One therefore takes a somewhat larger value of Θ at which the image gives a good compromise between intensity and contrast.

---

[2] For methods for the *surface* observation of Weiss domains (Bitter patterns, magneto-optical Kerr effect, etc.) see, for example, R. M. Bozorth, J. Phys. et Rad. **12**, 308, 1951 and B. W. Roberts, Conf. Magnetism and Mag. Mat., Pittsburgh, Pa., 14-16 June 1955, p. 192.
The method using the Faraday effect has also been used by P. A. Miles, who employed iron oxides of garnet structure as the transparent ferromagnetic (Prog. Rep. M.I.T. Lab. Insul. Res. **21**, 17, 1957).

is therefore minimized by a reduction of the number of domain walls per cm length, i.e. the domains become broader. This effect is strikingly demonstrated in fig. 3. This photo is analogous to fig. 2 but represents another region of the specimen. The platelet has here a terraced change in thickness which can be seen (owing to the increased absorption) as broad dark bands passing through the whole domain pattern. Inside the dark bands the Weiss domains are seen to be broader than in the lighter regions.

The elongated Weiss domains run continuously through the light and dark regions and apparently are not affected by the "steps" on the surface. To enable this continuity to occur, with a different number of domains per cm length in adjacent regions, some geometrical rearrangement is necessary. One can see how this occurs in the pattern; at the boundary of A and B, "extra" Weiss domains can be seen to end at various places on the boundary, showing a certain resemblance to edge dislocations in a crystal lattice. At one place on the boundary of B and C a region of meandering Weiss domains occurs, which serves to fill in a space which has arisen owing to the contraction of the domains in C.

Finally, a remark concerning the Faraday effect which is responsible for making the domain pattern visible. The Faraday effect in ferromagnetics has been known for some years, viz. in ferrites which are transparent to electromagnetic waves of centimetre and decimetre wavelengths. From the theory of the propagation of these waves in ferromagnetics, due to Polder ³), a rotation of the plane of polarization is to be expected in the presence of a suitable external magnetic field; this is a result of the interaction between the precessing electron spins (aligned by mutual interaction) and the rotating *magnetic* field of a circularly polarized wave with the right sense of rotation. This is the same interaction as causes ferromagnetic resonance. The Faraday effect in ferrites has been usefully applied in ferrite isolators for microwaves ⁴). One is tempted to attribute the Faraday rotation in $BaFe_{12}O_{19}$ at optical wavelengths, with which we are concerned here, to the same mechanism as that in ferrite isolators at microwave frequencies. This is not borne out quantitatively, however. A calculation of the rotation to be expected on the basis of magnitude of the spin-field interaction (known from other effects), results in a value about 100 times smaller than that observed. The Faraday effect in the present case must in fact be attributed to the interaction between the orbital electrons (whose orbits are aligned by the spin-orbit interaction in a ferromagnetic) and the rotating *electric* field of the circularly polarized light beam ⁵). This is essentially the same mechanism as that responsible for the normal Faraday effect with light waves in diamagnetics. In the ferromagnetic $BaFe_{12}O_{19}$ the effect is so strong that even a thickness of 1 micron provides an observable effect.

C. KOOY.

---

³) D. Polder, On the theory of ferromagnetic resonance, Phil. Mag. **40**, 99-115, 1949. See also H. G. Beljers and J. L. Snoek, Gyromagnetic phenomena occurring with ferrites, Philips tech. Rev. **11**, 313-322, 1949/50.

⁴) C. L. Hogan, The ferromagnetic Faraday effect at microwave frequencies and its applications. The microwave gyrator; Bell Syst. tech. J. **31**, 1-31, 1952.
A. G. Fox, S. E. Miller and M. T. Weiss, Behavior and applications of ferrites in the microwave region, Bell Syst. tech. J. **34**, 5-103, 1955. See also H. G. Beljers, The application of ferroxcube in unidirectional waveguides and its bearing on the principle of reciprocity, Philips tech. Rev. **18**, 158-166, 1956/57 (No. 6).

⁵) H. R. Hulme, Proc. Roy. Soc. **A 135**, 237, 1932.

BARIUM GETTER FILMS

by J. J. B. FRANSEN and H. J. R. PERDIJK.

621.385.1.032.928

During the many years of mass-production of electron tubes, a great deal of experience has been accumulated regarding the best methods of depositing the barium getter films, which serve to bind any residual or liberated gases. In spite of much research, however, it has hitherto not been entirely clear why one method is more efficient than another.

In the article below the authors put forward a hypothesis, based on a variety of experiments, concerning the structure of the barium getter films in most commercial valves and the manner in which the films occur. The hypothesis is very simple and makes it possible to give a straightforward explanation of the experimental results.

In electronic valves there must be no increase in the gas pressure during operation. The gases liberated in a radio valve cause the grid current to rise and can also lead to undesirable chemical reactions. A chemical reaction with the cathode can result in a drop in emission, and a reaction with the substances used for coating the grids changes the characteristics of the valve. Adsorption, too, at the surface of a grid can so alter the condition of the grid as to affect the valve characteristics. In a gas-filled valve any contamination of the gas will alter the ignition, burning and extinction voltages.

In order to limit as much as possible the increase of gas pressure in a sealed-off electronic valve, the components are subjected to a suitable pre-treatment, and during evacuation the valve is outgassed by heating to a high temperature, perhaps combined with electron bombardment. This does not, however, prevent the liberation of gases entirely. The gases in question are found to be mainly carbon monoxide and hydrogen, and to a lesser extent water vapour. In certain cases nitrogen, oxygen and carbon dioxide may occur [1]).

For the removal of these gases all valves are provided with an "internal pump", which goes on functioning during the whole useful life of the valve. This pump consists simply of a certain quantity of a substance (the getter material) which is capable of absorbing gases (usually a chemical binding is involved). To ensure that the process takes place quickly and in such a way that as much as possible of the getter material really remains active (it might, for example, become inactive merely owing to inaccessibility by being blocked off), it is usually necessary for the material to be applied in a special manner inside the valve envelope.

The substance first used for "gettering" was phosphorus. It is still used for this purpose in incandescent lamps, but in radio valves its place was soon taken by magnesium. Nowadays the getter materials most commonly used are barium (for radio valves and television picture tubes) and zirconium (for transmitting valves).

In this article we shall confine ourselves to barium. Before going into details concerning the technique of using barium as a getter material, it should be mentioned here that the metal is present in the finished valve or tube in the form of a thin film deposited on a part of the inside wall. With reference to some experiments which we have carried out we shall try to give a picture of the physico-chemical background of the rules, familiar in practice, governing the application of the barium film. The hypothesis underlying this picture is confirmed by electron-microscopic examination. It will also be shown what chemical reaction is, in all probability, responsible for the absorption of carbon monoxide.

First of all we shall consider some aspects of the techniques relating to barium getters.

The use of barium as a getter material

In the early period of barium getters the free element was usually introduced by suction into thin tubes of nickel, short lengths of which were mounted at an appropriate position inside the valve and heated after evacuation of the bulb. The barium vaporized and formed a thin deposit (the getter film) on the glass wall. This technique has now practically fallen out of use, mainly because the "packing" — the so-called getter holder — does not adequately protect the barium from spoiling in the time between its production and its employment in the valve.

---

[1]) Cf. S. Wagener, Vacuum 3, 11, 1953, where the various gases given off by different parts of a valve are mentioned. See also J. Peper, Philips tech. Rev. 19, 218-220, 1957/58 (No. 7-8).

Getter holders were subsequently developed containing a certain quantity of a barium compound which is not affected by contact with the air. At the present time the most widely used material is a barium-aluminium alloy in the proportion of one barium atom to four aluminium atoms. We shall therefore be concerned solely in this article with getter films originating from this alloy.

Types of getter holders

The form of a getter holder differs according to the amount of barium to be vaporized. If only small amounts are required, the holder is usually an iron tube with a top segment cut away and with a "stirrup" of nickel wire welded to both ends (see *fig. 1*). The closed circuit thereby produced enables the getter holder to be heated by means of high-frequency induction. The heating gives rise to a reaction in which the aluminium forms a bond with the iron and the barium escapes.

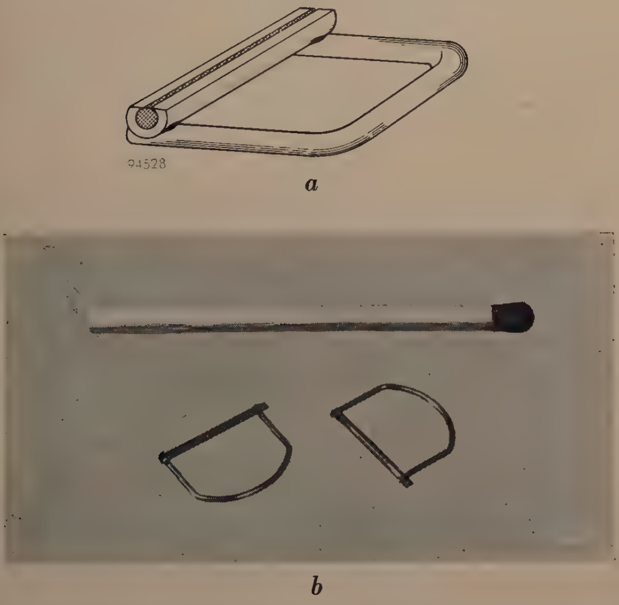

Fig. 1. *a*) Illustration of a getter holder having the form of a longitudinally ground-off tube. The "stirrup" welded to it makes it possible to heat the holder by induction.
b) Photograph of two such getter holders.

If greater quantities of barium are required, metal strips are used in which round depressions have been made at equal distances apart. Each depression is filled with a "pill" of the material supplying the barium. Short pieces of such strips, containing, say, two pills, can be made suitable for inductive heating by fitting them with loops as in the case of the iron tubes; longer strips can be bent into the form of a ring (*fig. 2*). In *figs. 3a* and *4* can be seen how the getter holders commonly used in a radio valve and television picture tube, respectively, are mounted on the electrode system.

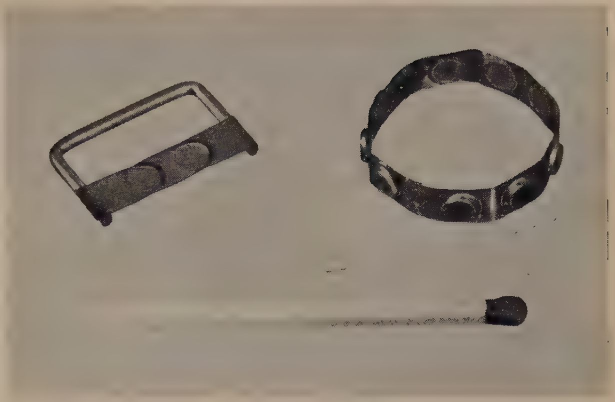

Fig. 2. Getter holders made from a metal strip with round equally spaced depressions containing barium "pills". For the purpose of induction heating a loop is welded to the getter shown on the left. The other consists of a longer strip bent to form a ring.

Vaporizing of the barium; "melt" curve

The barium that escapes from the heated getter holder settles on the neighbouring parts of the bulb wall. The resultant barium film is usually glossy in appearance and is about 1 μ thick. The film can be seen in fig. 3*b* which shows the same valve as in fig. 3*a* after vaporization of the barium.

The following points arise in connection with heating the getter holder. If a high power is applied, there is a risk that the holder will melt before sufficient barium has vaporized. On the other hand, if the h.f. power is only slightly higher than that necessary to start vaporization, quite small varia-

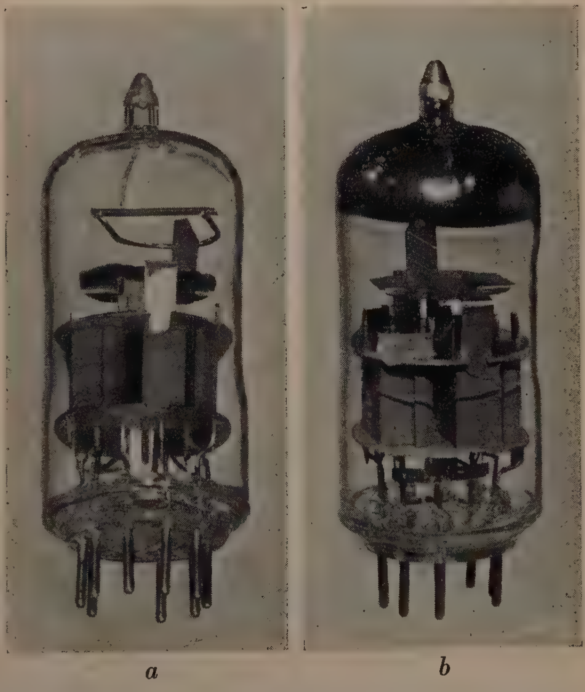

Fig. 3. Radio valve containing a getter holder of the type shown in fig. 1, *a*) before, and *b*) after vaporization of the barium.

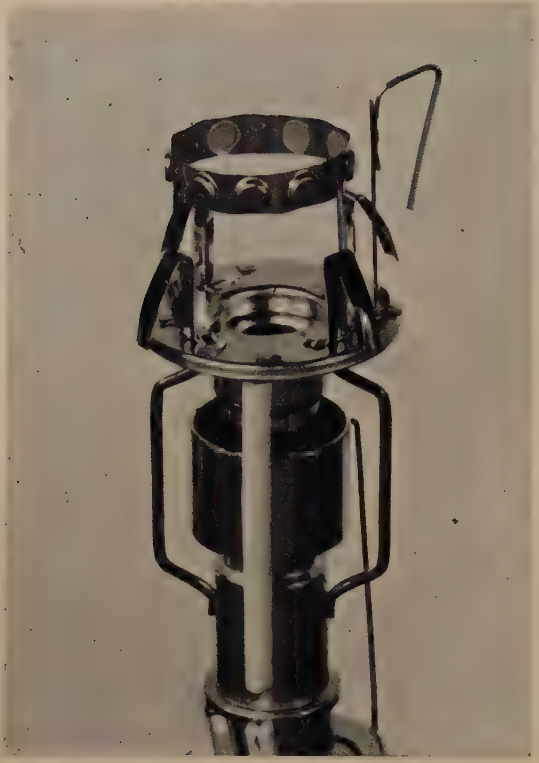

Fig. 4. Part of the electrode system of a television picture tube on which a ring-type holder (fig. 2) is mounted. To avoid any disturbing effect on the electron beam, the getter holder in television picture tubes is made of non-magnetic material.

tions both in the adjustment of the high-frequency generator and in the properties of the getter holder plus filling, will cause large variations in the quantity of barium vaporizing in a given time. Moreover, the barium will then, of course, vaporize very slowly, so that the process must be protracted. During this time the getter holder radiates considerable heat, which raises the temperature of the glass bulb; it will be shown below why this is not desirable.

The manner of heating can be represented by a point in a graph, the ordinate being the time t at which the first deposited barium becomes visible (this is a measure of the power supplied) and the abscissa the time T during which the getter holder is heated. In order to ascertain quickly whether a given combination of h.f. power and heating time is permissible having regard to the risk of melting, it has been found useful to plot a characteristic curve for each type of getter holder. This "melt" curve, as it may be called, is obtained as follows. Samples of the getter holder in question (barium-filled) are each heated by a different h.f. power, and a measurement is made of the above-mentioned time t and the value τ of the time of heating after which the holder melts. The behaviour of each sample is then marked by a single point in the graph, with τ on the abscissa and t on the ordinate (*fig.* 5). The envelope of the points having the higher values of t and the lower values of τ is then drawn, the resultant curve being the melt curve.

It is evident that working-points (combinations of t and T), so chosen that no melting occurs, will as a rule appear in the graph to the left of the melt curve. With the aid of such a graph one can quickly decide what the conditions should be to get the largest possible (and the least variable) fraction of the available barium to evaporate in a short time.

Absorption capacity and gettering rate

For defining the performance of a getter the terms absorption capacity and gettering rate are used.

The absorption capacity is the maximum quantity of gas that a given getter (here the barium film) is capable of absorbing.

The gettering rate a is defined by the formula:

$$\frac{\mathrm{d}Q}{\mathrm{d}t} = p\,a, \quad . \quad . \quad . \quad . \quad . \quad . \quad . \quad (1)$$

where the differential coefficient on the left side represents the quantity of gas absorbed (gettered) per unit time, and p is the gas pressure. The value of a depends on the nature of the absorbed gas as well as on the quality of the getter. It is customary to express p in microns Hg, Q in litre.microns [2]) and t in seconds. The gettering rate a is therefore expressed in litres per second and the absorption capacity, of course, in litre.microns (l.μ).

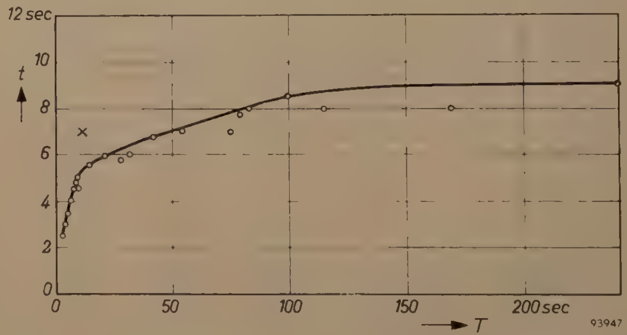

Fig. 5. "Melt" curve for the Philips getter holder R1 679 51. The time t at which the first barium deposit begins to form is plotted against the value τ of the heating time T at which the holder melts through. Each measurement is represented by one point, with τ on the abscissa and t on the ordinate. The higher the power applied, the smaller are t and τ. The envelope of the points representing the lower values of τ, is the "melt" curve. The graph gives the maximum permissible duration of heating at a given t (i.e. at a given applied power). The working-point for the experiments described below with this type of getter holder is marked by a cross in the figure (t = 7, T = 11 sec).

---

[2]) The comparison of quantities of gas solely be means of the product of volume and pressure is, of course, only feasible if the temperature remains the same. The numerical results reported in this article refer to room temperature.

It has been found that, to ascertain the quality of a barium getter film, it is necessary to define not only the above quantities, which relate to the whole film, but also corresponding quantities relating to one milligramme of barium and one cm² of the surface covered by the film. These specific quantities are respectively the absorption capacity per mg (unit: l.µ/mg), the absorption capacity per cm² (l.µ/cm²), the gettering rate per mg (l/sec.mg) and the gettering rate per cm² (l/sec.cm²).

Measuring the gettering rate

The set-up which we used for measuring the gettering rate is shown schematically in *fig. 6*. The barium getter film under investigation is contained in the bulb *C*, which is connected via a capillary *W* with the space *A*. The latter is connected via a "lock" *L* (consisting of stopcocks g_1 and g_2) to the gas reservoir *B*, and via a cooler *R* and a stopcock g_3 to the mercury-diffusion pump *P*. The pressure in *A* is measured by a Pirani gauge *M*; the lock *L* makes it possible to feed in a known quantity of gas.

The measurement was carried out as follows. Before forming the film, the spaces *C*, *A*, *R* and *L* were evacuated (g_3 open, g_1 closed). After the film had been formed, g_3 was closed and, by means of lock *L*, a quantity of gas was admitted into space *A*. From this moment onward, the pressure in *A* was measured, the gas present in *A* being able to flow via *W* to *C*, at a speed determined by the resistance of *W* and by the pressure in *C*, that is by the rate at which the getter film absorbed the gas entering *C*.

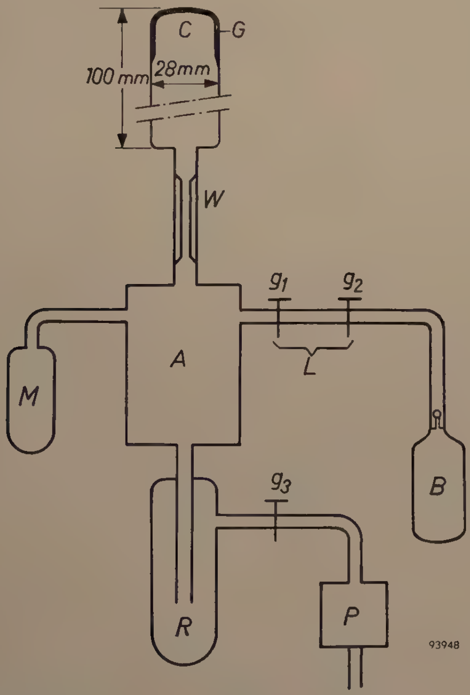

Fig. 6. Set-up used for measuring the "gettering rate" of a barium getter film. A constant quantity of the gas in *B* is admitted to *A* via the lock *L*, consisting of stopcocks g_1 and g_2. Via the capillary *W* the gas flows into the bulb *C* containing the barium getter film *G*. The time-variation of the pressure in *A*, measured by a Pirani gauge *M*, is governed by the permeability of the capillary *W* and the gettering rate to be measured.

Writing the pressures in *A* and *C* as p_1 and p_2 respectively, the total volume of *A*, *R*, *L* and *M* as V_1, the volume of *C* as V_2, the conductivity of *W* as *F*, the time as *t* and the gettering rate as *a*, we can describe what happens in terms of the following equations:

$$V_1 \frac{\mathrm{d}p_1}{\mathrm{d}t} = -F(p_1 - p_2), \quad \ldots\ldots \quad (2)$$

$$V_2 \frac{\mathrm{d}p_2}{\mathrm{d}t} = F(p_1 - p_2) - a p_2. \quad \ldots\ldots \quad (3)$$

When $V_1 \gg V_2$, so that V_1 and $(V_1 + V_2)$ can both be put equal to *V*, and when *a* and *F* are constant, the solution is:

$$p_1 = p_0 \exp \frac{-t}{(1/a + 1/F)V}, \quad \ldots\ldots \quad (4)$$

$$p_2 = \frac{p_0}{1 + a/F} \exp \frac{-t}{(1/a + 1/F)V}, \quad \ldots \quad (5)$$

where p_0 is the initial value of p_1. As stated, the pressure in *A* was measured as a function of time. From equation (4) it follows that the logarithm of the measured p_1 plotted against *t* will produce a straight line. If the amount of gas admitted is sufficiently small, this is indeed found in the course of a single continuous measurement. A family of such curves, obtained from measurements with hydrogen, is given in *fig. 7*. It can be seen that *a* becomes smaller according as more gas has been absorbed by the getter film.

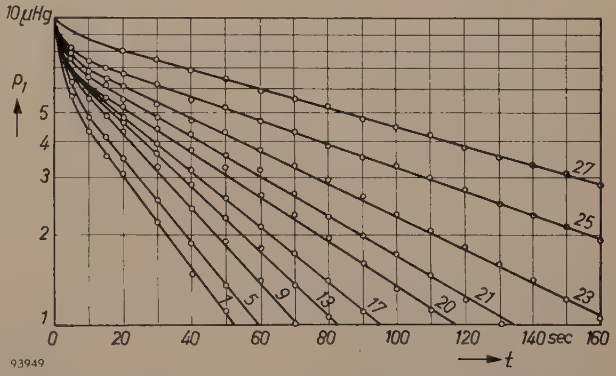

Fig. 7. Gettering rate for hydrogen measured on a single barium film, the logarithm of the pressure p_1 being plotted against the time *t* which has elapsed since the admission of a given quantity of gas. After a short time the relationship is linear. As more gas is absorbed the gettering rate decreases and the curve becomes less steep. The curves represent the pressure gradient after the first, fifth, ninth, etc. admissions of gas.

The quality of a barium getter film in relation to its structure and manner of preparation

The quality of a barium film as a getter depends on many factors and is by no means exclusively determined by the quantity of barium which it contains or by the surface area of the glass wall covered by barium. Besides such factors as the form of the getter holder, the quantity of barium in it, whether or not it has been subjected to prior outgassing and the method of heating it when vaporizing the barium, an important part is played by the temperature of the bulb, the distance of the getter holder from the bulb wall and the presence of gas in the valve during the vaporizing process.

In experimental investigations on the influence of each of the above factors it is, of course, necessary to keep the others as constant as possible. With factors such as the temperature, the means of arranging this are fairly obvious, and no special description is required. Others, such as the shape of the holder, can certainly be kept constant within a series of experiments but the precise conditions are difficult to describe, for which reason they are treated rather cursorily in some publications. The outcome is that the results reported in these publications can hardly be compared quantitatively with others 3).

In view of the experiments described in this article and in the light of the experience which we and others have gained with barium getter films, we believe that the production of a barium film and its structure should be regarded as taking place in the following way.

When the getter holder, with its barium-containing material, is heated to the temperature for vaporizing the barium, not only does the barium escape but gases are liberated as well, it not being possible to outgas the getter holder completely. There is reason to assume that, in consequence of this, the barium does not fly in atomic form from the getter holder to the bulb wall but rather as a "mist" composed of minute droplets. The diameter of these droplets is determined in the immediate vicinity of the holder.

The mechanism of this process may well be such that fairly numerous collisions take place near the getter holder between gas molecules and barium atoms, whereby droplets of barium condense from the vapour to form the mist described 4). There are other arguments, however, for the view that the barium is already in the form of droplets upon leaving the holder.

At all events, a barium getter film produced from such a mist will consist of a porous structure of stacked round grains of barium. The "microscopic" surface of this film is larger (per mg barium) according as the barium grains are smaller and less fused together. They will fuse together less, the lower is the temperature of the bulb and of the droplets at the moment of arrival.

Photomicrographs, made with an electron microscope, of the surface of barium getter films support this hypothesis (*fig. 8*). The surfaces of two films containing respectively 0.9 and 2.6 mg barium (over an area of 35 cm^2) are seen to have a grainy structure. The surface of the third film, containing 3.5 mg barium, gives the impression of being formed by grains which have partly fused together. The grains visible on the micrographs of the first two films have a diameter of about 0.04 μ 5).

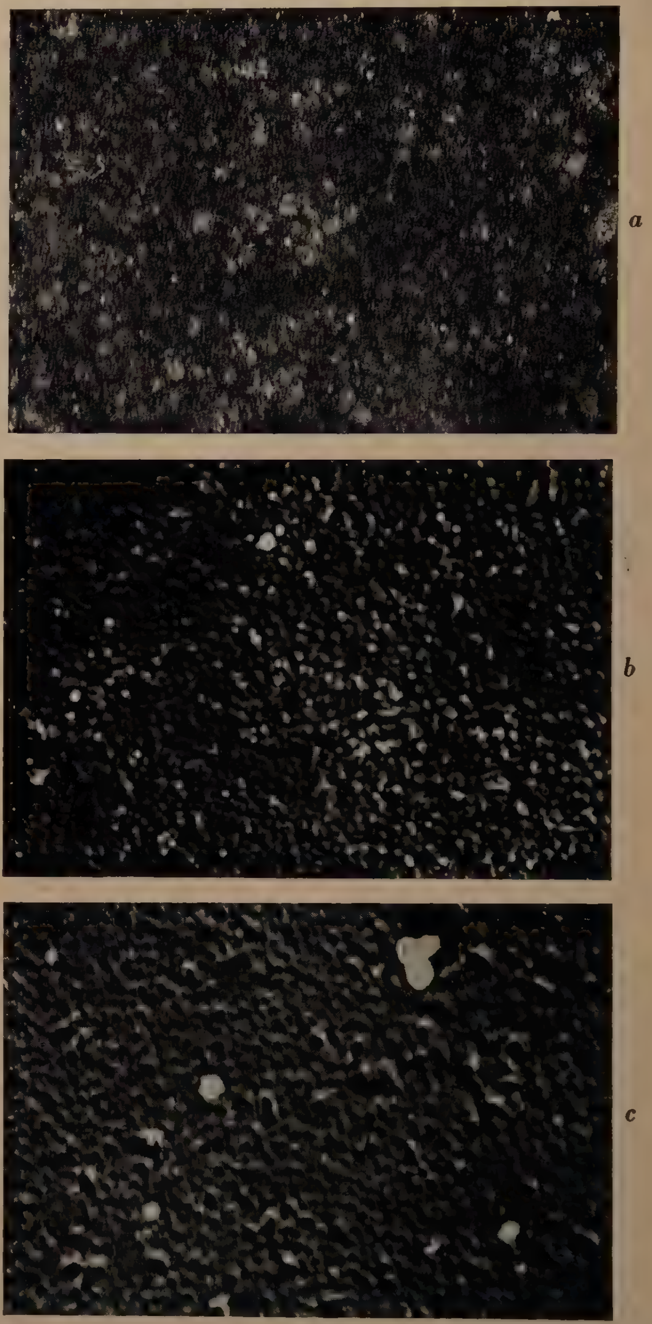

Fig. 8. Photomicrographs made with an electron microscope, of SiO replicas of the surface of barium films having a macroscopic area of 35 cm^2 and containing respectively 0.9, 2.6 and 3.5 mg barium. Magnification 80 000 $\times$.
a) Surface of film containing 0.9 mg Ba, exhibiting more or less spherical grains with a diameter on the photograph of approx. 3 mm; the actual grain diameter is thus about 0.04 μ.
b) and *c*) Surfaces of films containing respectively 2.6 and 3.5 mg Ba. The grains are still clearly distinguishable, but are now somewhat fused together, particularly in *c*.

---

3) For example, observations by Wagener (Vacuum **3**, 11, 1953) of the absorption of hydrogen conflict with those by Della Porta (Vacuum **4**, 284, 1954). Our results are complementary to those of the former author.

4) See J. E. de Graaf and H. C. Hamaker, Physica **9**, 300 and 301, 1942 and Y. Mizushima, Z. Oda and O. Ochi, J. Phys. Soc. Japan **12**, 365, 1957 (No. 4).

5) These photomicrographs were made by H. B. Haanstra of Philips Research Laboratories.

For examination with the electron microscope it is, of course, necessary to use a replica technique, such that the replica of the barium film can be formed in the evacuated valve. A method was adopted whereby a thin SiO film was vapour-deposited on the object [6]. The Si-SiO_2 mixture, which was heated to produce the SiO, was placed in a container of conically wound tungsten wire. Before vaporizing the barium, the container with its contents was thoroughly outgassed.

The barium films investigated were identical as regards the manner in which they were deposited with those on which we carried out experiments with CO to determine the influence of wall temperature. We shall discuss these experiments presently.

Influence of the getter holder; gettering-rate measurements with hydrogen

Our view that the properties of a barium getter film are largely established when the barium is still close to the getter holder, is based on gettering-rate measurements with hydrogen.

From the first series of measurements it was found that the rate with which a barium film absorbs hydrogen, as long as the film is not yet saturated, decreases linearly with the quantity of the gas already absorbed. By drawing a straight line through the values found, and extrapolating, we find the value of the initial gettering rate a_0 from the point of intersection with the gettering-rate axis. The point of intersection with the other axis gives the capacity of the film. The results of such a series of measurements, plotted in this manner, are shown in *fig. 9*. Variation of the amount of gas admitted produced no significant change in the value found for a_0, which indicates that, for the absorption of hydrogen, a_0 is constant in a fairly wide pressure range (the initial pressure varied from 10 to 100 μ Hg).

The value found for the initial gettering rate per mg barium was $(2.5 \pm 0.2) \times 10^{-2}$ l/sec.mg. (The quantity of barium in the films varied from 6.3 to 7.9 mg. The area of the films was in every case 35 cm^2, which means that if the barium were to form a solid, smooth layer, the thickness would be between 0.49 and 0.61 μ.)

In the second series of measurements the inside of the bulb was given a prior coating of colloidal graphite, producing a rough surface. If the barium film were a smooth homogeneous layer, the area of the barium film exposed to the gas, and hence the initial gettering rate, would now necessarily be larger than if the film were deposited on a smooth glass wall. It was found, however, that under these conditions the initial gettering rate per mg was the same as in the first series of measurements [7]).

In the third series of tests the getter holder was mounted in a large glass sphere, so that the film deposited had a substantially larger macroscopic area (186 cm^2) than in the first two series. The thickness was, of course, proportionally smaller and was approximately constant over the whole surface. Here again the same value was found for the initial gettering rate per mg.

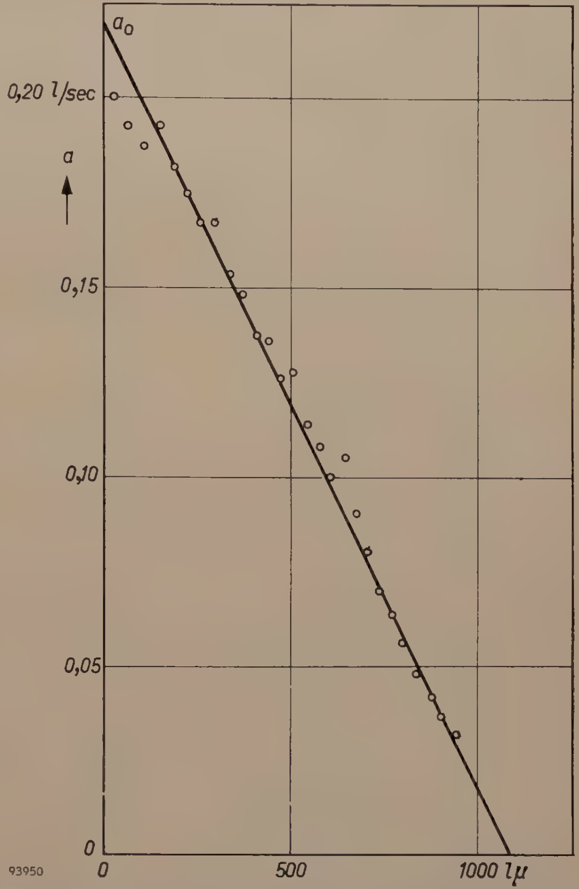

Fig. 9. The absorption of hydrogen by barium shows the appearance of a volume effect: the absorption rate (ordinate) depends linearly on the amount of gas already absorbed (abscissa). Extrapolation of the line drawn through the measured points gives the initial rate (point of intersection with vertical axis) and the total absorption capacity (point of intersection with horizontal axis).

It may be concluded, then, that in all the three cases mentioned the area of the film accessible to gas (the "microscopic area") was equally large, which is in agreement with our picture of the film as a porous structure of stacked barium spheres: for, the number and magnitude of the spheres may be assumed to be equal in all three cases.

---

[6]) See G. Hass and N. W. Scott, J. Opt. Soc. Amer. **39**, 179, 1949.

[7]) J. Morrison and R. B. Zetterstrom, J. appl. Phys. **26**, 437, 1955, carried out an analogous experiment with MgO instead of graphite. As in our case, they found for CO no greater values for a_0 nor for the absorption capacity.

In addition it was found that the gettering rate is proportional to the total quantity of the barium not yet used up; a linear relationship exists between a and the quantity of gas already absorbed. The absorption of hydrogen thus shows the appearance of a volume effect [3]).

In the fourth series of measurements, using the same large bulb mentioned above, a combination was introduced of two or three of the strip getters used in the first three series. It was found in this case that a_0 itself as well as the initial gettering rate, related to one cm^2 or to one mg, had both decreased. With two strip getters the latter had dropped to about $^1/_5$, and with three strip getters to as little as about $^1/_{25}$ of the value of the first three series; a_0 itself had dropped to about $^1/_2$ and $^1/_5$ respectively of the former values. The film thickness in the tests with three strips was the same as in the first series; in the tests with two strips it was slightly less than half.

The fact that, in spite of variation in the film thickness, a constant value was found for the initial rate per mg in the first three series, whereas a different value was found when using different getter holders (in the fourth series), demonstrates that the properties of a getter film are partly determined beforehand in the immediate neighbourhood of the getter holder, and depend upon the type of holder used.

Experimental details. The barium getter films investigated in the above four series were obtained from samples of the Philips strip getter type R1 679 36, illustrated in fig. 2. To minimize variations in properties, the getters were taken from a single production run. (This was also done for all subsequent experiments.) High-frequency outgassing was not applied, but for all tests the bulb and getter holder were heated at 400 °C as soon as high vacuum was reached. The barium getter film was allowed to form as soon as the bulb had cooled to room temperature.

During the formation of the film the temperature of the bulb rose slightly owing to the barium cooling on it and to the heat radiated by the glowing getter holder. The differences in this respect between the small and large bulbs did not appear to be significant. The gettering-rate measurements were always carried out after the bulb had dropped to room temperature again. *Fig. 10a* shows the getter holders used in the fourth series of tests.

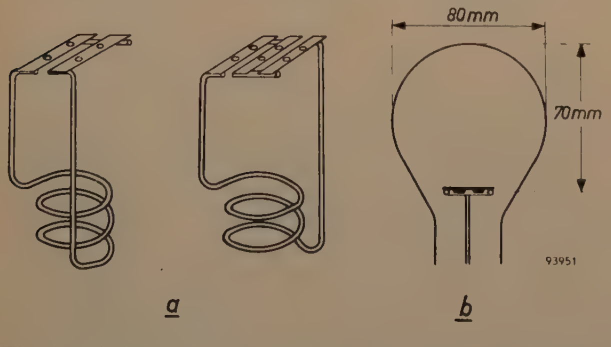

Fig. 10. *a*) Getter holders made by combining two and three strips, respectively, and provided with a coiled support for induction heating.
b) Sketch showing dimensions of the large bulb used for making a getter film of large macroscopic area and constant thickness.

The dimensions of the small bulb are indicated in fig. 6, those of the large bulb in fig. 10*b*. In the large bulb, the getter holders were so positioned as to produce getter films of as constant a thickness as possible and with well-defined edges.

Influence of the wall temperature; measurements of absorption capacity for CO

The size of the microscopic surface of barium getter films can be comparatively investigated not only by measurements of the gettering rate, as described above, but also — and more simply — by measurements of the *absorption capacity*, provided a gas is used which is known with certainty to be absorbed by the *surface*. Such a gas is carbon monoxide [8]).

According to our hypothesis regarding the structure of the barium films and the manner in which they are formed, we may expect that a film of this kind will show the following properties. In the first place the absorption capacity for CO will decrease according as the temperature of the bulb wall was higher during the deposition of the film. In the second place the absorption of a film which is so sparse that the barium grains lie separate from each other (i.e. cannot fuse together) will be large and will not be greatly affected by the temperature of the bulb during the formation of the film.

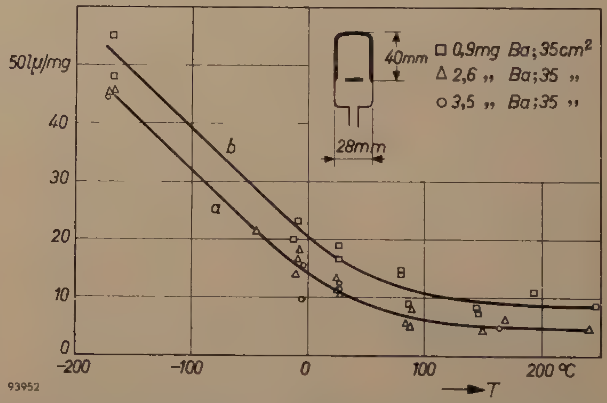

Fig. 11. Measurements of absorption capacity for carbon monoxide. The absorption capacity per mg barium, measured at room temperature, is plotted against the temperature of the bulb during the formation of the barium film. In all cases the getter holder was 40 mm away from the end of the tube. The values found for films containing 3.5 and 2.6 mg barium show no significant difference (curve *a*). Curve *b* applies to films containing only 0.9 mg barium.

The first-mentioned effect is clearly demonstrated in curve *a* of *fig. 11*. In this figure the absorption capacity per mg — all measurements, as with hydrogen, at room temperature — is plotted against the temperature of the bulb wall for two kinds of film (containing respectively 3.5 and 2.6 mg barium and originating from two types of getter holders). It is striking that the values found with both kinds of film coincide within the accuracy of measurement and are higher the lower was the temperature.

---

[8]) See S. Wagener, J. phys. Chem. **60**, 567, 1956.

The properties of films so sparse that the barium grains lie separate from each other (obtained from a third type of getter holder), appear from the measurements represented by curve *b* in fig. 11 and by *fig. 12*. The measurements first mentioned were made on films which were transparent over a part of their surface (0.9 mg Ba on 35 cm^2), which was not the case with the films represented by curve *a*. The variation of absorption capacity with temperature is completely identical with that of curve *a*, but all values are somewhat higher; this is understandable if we assume that the barium grains lie free in the transparent part of the film.

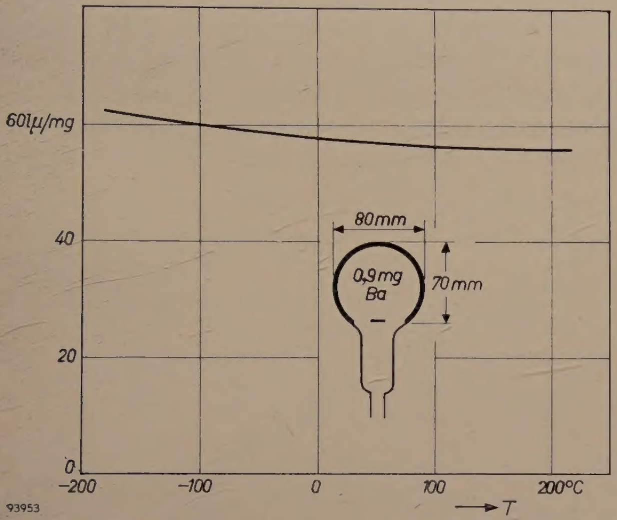

Fig. 12. Absorption capacity per mg of barium films whose grains are not in contact with each other. It can be seen that in this case the temperature of the bulb wall during the formation of the film has only a negligible effect on the absorption capacity.

The measurements recorded in fig. 12 were made on extremely thin films (0.9 mg Ba on 262 cm^2). We see that in fact the absorption capacity per mg is again larger than found by the measurement recorded by curve *b* in fig. 11. Furthermore the absorption capacity, as expected, is here almost independent of the temperature of the bulb wall during the formation of the film.

Experimental details. The above experiments with CO, and some others still to be discussed, were carried out with getter holders of three different types (Philips Rl 679 50, Rl 679 51 and Rl 679 82). They were heated for a time T of 11 sec, the "vaporizing time" t being 7 sec [9]). A number of measurements showed that the quantities of barium vaporized under these conditions were respectively 3.5 ± 0.2 mg, 2.6 ± 0.1 mg and 0.9 ± 0.1 mg.

The set-up for these measurements (see *fig. 13*) differed slightly from that used for the hydrogen experiments. The quantity of gas (coming from the reservoir B via the lock L formed by the stopcocks g_1 and g_2, and further via the three-way cock g_4 and the liquid-air traps R_1 and R_2) which was admitted to the barium film G, was in this case determined beforehand by a pressure measurement with a MacLeod gauge M. The extra trap R_2 was put in operation after outgassing of space C (heating to 400 °C) and before the depositing of the barium film. This was always done in those experiments whereby the space C was at a temperature below room temperature, and frequently also in the other cases for test purposes.

In the experiments on the influence of the bulb temperature the distance from the getter holders to the apex of the bulb was invariably 40 mm, and the area covered by barium was in all cases 35 cm^2.

Further experiments with CO

It has long been known that very good getter films are obtained when the valve in which the getter is vaporized is filled with an inert gas under suitable pressure [10]).

In order to compare the quality of these films quantitatively with that of others, we performed a number of experiments the conditions of which, apart from the gas filling of the valve, were identical with the experiments discussed above on the influence of the bulb temperature. The valve was filled with argon under a pressure of 6 mm Hg.

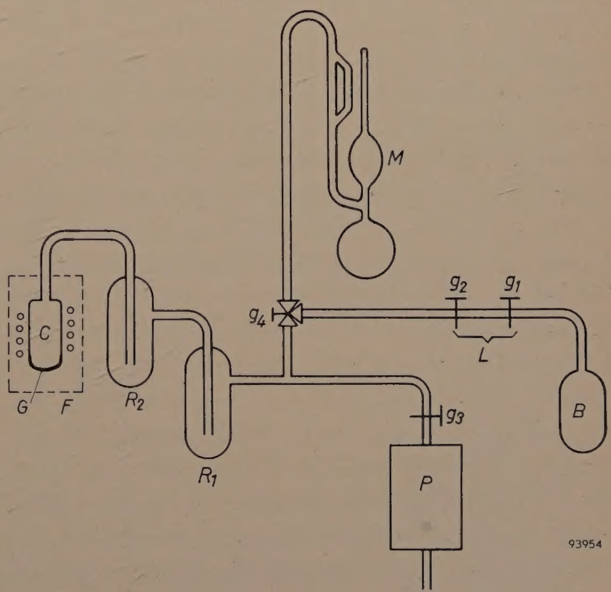

Fig. 13. Set-up used for measuring the absorption capacity for carbon monoxide. The letters have the same meaning as in fig. 6. The amount of gas admitted to C can be accurately controlled by the three-way cock g_4 and the MacLeod gauge M. The extra liquid-air trap R_2 was found necessary in those experiments in which the bulb wall was at a temperature lower than room temperature. F represents the heating or cooling device, as the case may be.

---

[9]) See page 292.

[10]) A. L. Reimann, Phil. Mag. **18**, 1117, 1934. See also the article by De Graaf and Hamaker, quoted under [4]).

The absorption capacity per mg was found to be not much larger than that found in the earlier experiments with very thin films.

This leads to the conclusion that the use of this gas filling does not essentially improve the properties of a barium getter film; on the contrary, under normal circumstances the best results are frequently not obtained, that is to say the mist of barium droplets is not deposited on the bulb in the most effective way.

Vaporization in a gas atmosphere gives rise, as a rule, to a black getter film. If the gas pressure is relatively low, a "normal" film is produced, which however also exhibits a large absorption capacity for CO. It is evident from the above, therefore, that there is no justification in regarding black getter films as belonging to a distinct class as regards their microscopic area. As mentioned earlier, the getter films of commercial electronic valves may be regarded effectively as vaporized through gas.

On the basis of our hypothesis on the structure and manner of formation of a barium getter film, which is confirmed by the experiments described, it is possible to explain the results of the following more complicated experiments. First of all a series of experiments was carried out in which the distance from the getter holder to the bulb wall was varied. Two distances were adopted, the getter holder being mounted 6 and 40 mm away from the apex of the bulb. The getter holders used in these experiments were the types earlier mentioned (yielding respectively 3.5 mg, 2.6 mg and 0.9 mg barium), so that we were able to make six types of getter film. During the evaporation of the barium the tube was neither heated nor cooled. Four of the six kinds of film were found to have almost the same absorption capacity for carbon monoxide per mg barium (12 l.µ/mg). The 3.5 mg film at a wall-to-holder distance of 6 mm was poorer (8 l.µ/mg), the 0.9 mg film at a wall-to-holder distance of 40 mm was better (18 l.µ/mg). In the first of these two cases a great deal of barium was present per cm^2 with the intensively radiating getter holder at a short distance from the bulb wall. In all probability this caused, during the vaporization, greater heating of the bulb and of the barium already deposited than in the other experiments. As we found earlier, this indeed results in a reduced absorption capacity. In the second case just the opposite was the case.

A further noteworthy result is that the same absorption capacity per mg is found for the 2.6 mg films at both wall-to-holder distances, although the films differ by a factor of 4 in surface area. This accords entirely with what we found earlier with regard to the absorption rate for hydrogen when the barium was vaporized in a small and in a large bulb. This result adds support to the view that measurements both of the gettering rate for hydrogen and of the absorption capacity for carbon monoxide can give a (relative) measure of the size of the area accessible to gas. The size of this "microscopic" area is evidently substantially independent of the macroscopic area of the film.

The following series of experiments which we shall discuss to conclude this section are a repetition of the earlier experiments on the influence of the bulb temperature, but now made with the getter holders (again the same three types) at a distance of only 6 mm (instead of 40 mm) from the bulb wall. The results are set out in *fig. 14*, with curve *a* from fig. 11 included for comparison. It can be seen that, as opposed to the curves in fig. 11, the absorption capacity per mg in this case tends to a maximum at wall temperatures below about —80 °C.

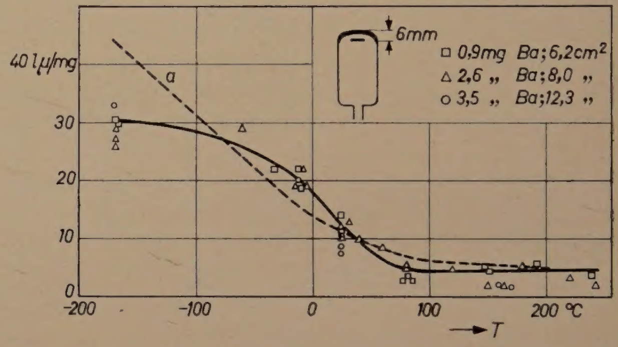

Fig. 14. Absorption capacity per mg of thick barium films as a function of the wall temperature during formation of the film. As in fig. 11, the plotted points refer to films containing 3.5 mg, 2.6 mg and 0.9 mg barium. The full curve is drawn to fit the points for the 0.9 mg films, but also applies fairly well to the others. Curve *a* from fig. 11 (dashed) is included for comparison.

This is due in all probability to the intense heat radiation from the getter holder. The fact that the values found at lower wall temperatures are also appreciably lower than in the earlier experiments points in the same direction. It is remarkable that between —80 °C and room temperature the absorption capacity per mg is higher than that of the thinner films of fig. 11. This is presumably caused by the action of the gas escaping from the getter holder during vaporization, because curves relating to later experiments with getters largely outgassed beforehand do not show this "hump". It appears from this that the position of a getter holder which has not been outgassed affects the quality of the film in an even more complicated way than could be deduced from the earlier experiments; the action of the gases released from the getter holder is apparently not exclusively determined by the method of heating and the nature and quantity of these gases.

If the absorption capacities measured in these experiments be considered not with respect to the quantity of barium but with respect to the macroscopic size of the film surface, it is found that at high temperatures the absorption capacities per cm² of all three kinds of film approach one and the same limiting value (approximately 0.5 l.μ/cm²). Remarkably enough, this value is higher than that found in the experiments of fig. 11 which was about 0.3 l.μ/cm² (getter holders at a distance of 40 mm from the bulb wall); see *fig. 15.* The reason for this may be the thin spreading-out of the film edges: in the experiments to which fig. 11 refers, the edges of the films were much more sharply defined and therefore less troublesome. In view of the dimensions involved, this thin spreading-out of the films might well be a consequence of the escape of gases during the vaporization of the barium.

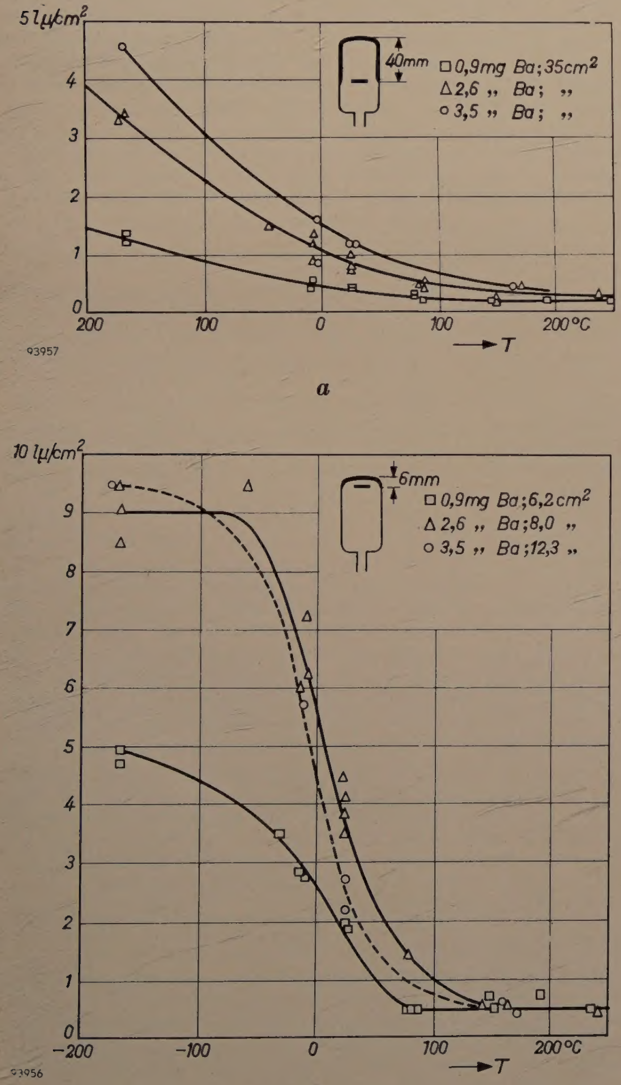

Fig. 15. *a*) Absorption capacity per cm² (macroscopic area) of the films for which the capacity per mg is given in fig. 11. *b*) Idem for the films in fig. 14.

Reaction of barium with carbon monoxide; calculation of grain diameter

According to Morrison and Zetterstrom [11]), barium may react with carbon monoxide in one of the following three ways:

$$\begin{aligned} \mathrm{Ba} + \mathrm{CO} &\rightarrow \mathrm{BaO} + \mathrm{C}, \\ 3\,\mathrm{Ba} + 2\,\mathrm{CO} &\rightarrow \mathrm{BaC_2} + 2\,\mathrm{BaO}, \\ \mathrm{Ba} + 2\,\mathrm{CO} &\rightarrow \mathrm{Ba(CO)_2}. \end{aligned}$$

From the results of some experiments now to be described it is our conclusion that it is the second of these reactions that actually takes place.

A barium film was deposited (at room temperature) in a bulb which had previously been heated to 400 °C. After raising the film to a temperature of 320 °C, a quantity of CO was admitted into the bulb. As soon as the film was saturated [12]), the CO that had not been absorbed was removed and water vapour admitted. Examination of the bulb contents with a mass spectrometer revealed that a chemical reaction had taken place: apart from water vapour, C_2H_2 was present. This gas could not have arisen if the barium and carbon monoxide had reacted according to the first or the third of the above three equations. It can, however, arise from the BaC_2 formed in the second reaction, according to the equation:

$$\mathrm{BaC_2} + \mathrm{H_2O} \rightarrow \mathrm{BaO} + \overset{\nearrow}{\mathrm{C_2H_2}}.$$

If we calculate how much CO can be absorbed by one mg barium in the second of the above three equations, we find 81.9 lμ. The result obtained from a number of experiments was 81 ± 7 lμ. This, too, indicates that the absorption takes place according to the second reaction.

Naturally this is still no proof that the said reaction is also responsible for the CO absorption at room temperature. We have reason to assume, however, that this is in fact the case: in the first place because of the fact that films with a large microscopic area exhibit the same change of appearance in the case of absorption of CO at room temperature (they become transparent with a light brown colouring), and secondly because of provisional results of a mass-spectrometer investigation now under way [13]).

---

[11]) See page 440 of the article quoted under [7]).

[12]) The temperature of 320 °C is high enough to ensure the reaction of all the barium and at the same time far enough below the temperature at which the bulb was outgassed (400 °C) to prevent the release of unwanted gases from the bulb wall.

[13]) These results will be published in due course elsewhere. Bloomer, Brit. J. appl. Phys. **8**, 352, 1957 (No. 9), believes that the reaction takes place according to the first of the above three equations.

It is expected that this investigation will explain, among other things, why, in our experiments, H_2 and CH_4 (and no C_2H_2) are formed when water vapour is admitted to barium getter films saturated with CO at room temperature. Such reactions with water are a possible reason for the fact that hydrocarbons are sometimes found in the residual gas (the gas not absorbed by the getter film) in radio valves.

A barium getter film "saturated" with CO at room temperature is also unable to absorb any further hydrogen or nitrogen, unless the temperature is raised. In this case an occlusive layer has apparently formed on the surface. Starting from the second reaction equation mentioned above and the lattice constant of barium (5×10^{-8} cm), we can calculate the thickness of this layer if we are able to measure the absorption capacity of a film whose active surface area is equal to the macroscopic area. This is the case with the films formed at a high bulb temperature. The limit value found here was approx. 0.3 l.μ/cm^2 (cf. fig. 15). It follows, then, that the layer in question contains about 36 atomic planes, i.e. its thickness is about 18 lattice spacings $= 9 \times 10^{-3}$ μ[14]). (The barium lattice is body-centred cubic.)

Diameter of the barium grains

If we assume that the result just found is also applicable to the grains from which we imagine a barium getter film to be composed (the grains not being fused together), we can calculate the diameter of these grains in the following way.

Let D be the average diameter of the grains, and d the diameter of that interior part of the grain which is inaccessible once the layer has formed, then the non-reacting fraction of the quantity of barium is $\frac{1}{6}\pi d^3/\frac{1}{6}\pi D^3$. On the other hand, from the measurements of the absorption capacity at 320 °C (about 81 l.μ/mg) and at room temperature (approximately 57 l.μ/mg for the extremely thin film mentioned earlier) we know that this fraction is about 24/81. A second relation between d and D follows from the known thickness of the layer: $D - d = 2 \times 9 \times 10^{-3}$ μ. The value of the grain diameter D found by solving these two equations is roughly 0.05 μ. If we take for the absorption capacity at room temperature the value found for the films formed in an argon-filled bulb (approx. 70 l.μ/mg), we find D to be about 0.04 μ. Both values are in good agreement with those which we derived from the photomicrographs obtained with the electron microscope. Assuming the diameter to be 0.05 μ, we then find that one mg barium is divided into 4.13×10^{12} grains. These have a total (microscopic) area of 325 cm^2 and would cover, if laid side by side in one layer, a wall area of 89 cm^2.

When applying in practice the results reported in this article it is necessary first of all to ascertain what gases are to be absorbed by the barium getter film. The absorption capacity for hydrogen and oxygen depends on the total quantity of barium, that for carbon monoxide on the size of the microscopic area. We have found that circumstances can arise in which a larger microscopic area is obtained when less barium is vaporized.

It has been found that better results are obtained as regards gettering rate (and also as regards the absorption capacity for CO) when the barium is vaporized after the tube has been sealed off and is at room temperature, than when the tube is still on the vacuum pump. This may also be explained in the light of the results given above.

Summary. The properties of the barium film deposited in vacuum tubes in order to absorb gases released after the tubes have been sealed off, depend in a complicated way on the manner in which the film is formed. The influence of the method of formation can be understood by assuming that the film consists of a stacked structure of barium grains partially fused together. It is suggested that these minute grains are solidified droplets of barium which are created not on the surface on which the film is deposited but in the immediate vicinity of the getter holder upon vaporization of the barium. The authors attribute this to the presence of gases escaping from the getter holder together with the barium. Experiments concerning the gettering rate for H_2 under various conditions all point in this direction.

The colder the wall on which these droplets are deposited, the less will they fuse together and the larger will be the "microscopic" area of the barium film. This is confirmed by experiments on the absorption capacity at room temperature for CO (a gas which is absorbed only at the surface). Films that are so thin that the spheres are not in contact with each other — and hence cannot fuse together — show a high absorption capacity for CO. As expected, the absorption capacity in this case is but little dependent on the temperature of the bulb wall during vaporization.

Films formed in valves containing argon (under 6 mm Hg pressure) have a high absorption capacity, although it is not much higher than that of the best "normal" getter films. It is concluded from this that vaporization in argon does not essentially improve the quality of a getter film, but rather that with "normal" vaporizations the best results are not as a rule obtained, i.e. the barium mist is not deposited on the wall in the most effective manner. Photomicrographs of an SiO replica of the surface of barium films, made with an electron microscope, show that the surface is indeed composed of small grains, which have a diameter of about 0.04 micron.

The absorption of CO takes place in all probability according to the reaction $3\,Ba + 2\,CO \rightarrow BaC_2 + 2\,BaO$. On this basis it can be calculated that the barium layer so transformed is about 18 lattice spacings thick, i.e. 9×10^{-3} μ. From this thickness, from the absorption capacity of a good barium film at room temperature, and from the absorption capacity of the same quantity of barium at 320 °C (at which temperature all the barium reacts), the grain diameter is calculated to be 0.04 to 0.05 μ.

In order to describe the properties of a barium getter film in more detail than hitherto, the authors introduce, in addition to the quantities gettering rate and absorption capacity, corresponding specific quantities with respect to both one mg barium and one cm^2 of the barium-covered surface.

The quantities vaporization time and heating time are introduced to characterize the way in which the getter holders are heated to vaporize the barium; the "melt" curve indicates the moment at which heating must be stopped to prevent the getter holder from melting.

---

[14]) Wagener, J. phys. Chem. **60**, 567, 1956, finds 27 atomic layers, i.e. 13½ lattice spacings.